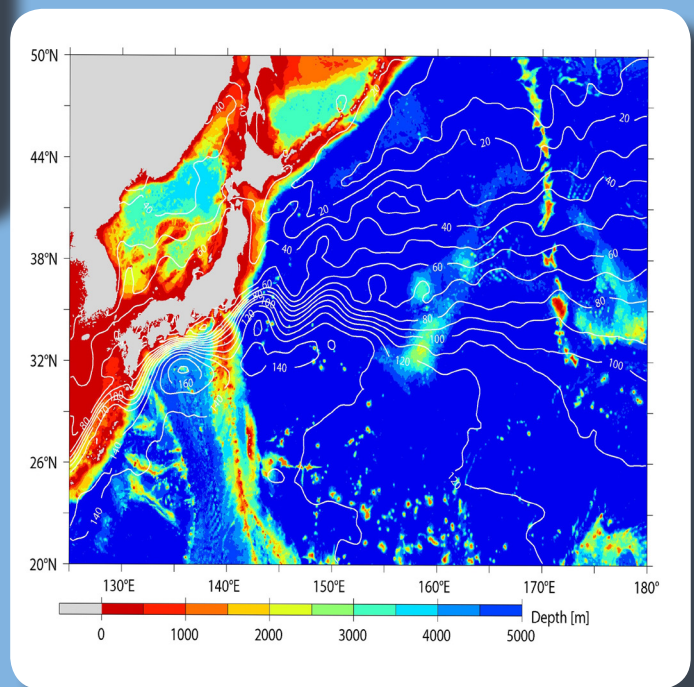
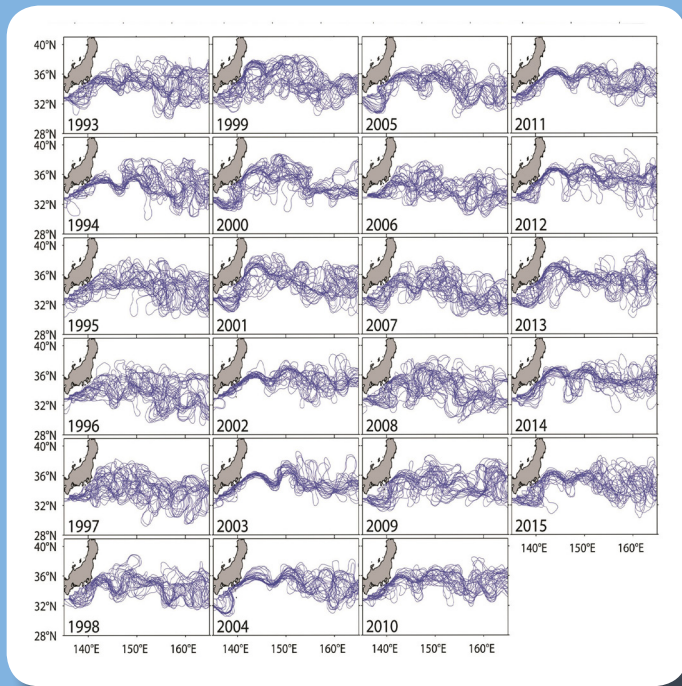


Special Issue: the Kuroshio Current and Extension System



Top: the semi-monthly Kuroshio/KE paths in years 1993-2015 based on satellite altimeter data, revealing the stable vs. unstable dynamical states of the Kuroshio/KE system. **Bottom:** the regional bottom topography (in color) and surface dynamical topography (in white contours) surrounding the Kuroshio and KE (courtesy of Bo Qiu, University of Hawaii).

Editorial

Nico Caltabiano

International CLIVAR Project Office, Southampton,
UK

The scientific community working on the Kuroshio Current and Extension has been very active for many years. This shows the importance of this system and its impact on climate, storm tracks, and ocean ecosystems. This issue of Exchanges highlights some of the latest findings on the Kuroshio System that were presented at another successful workshop organised by the CLIVAR Ocean Model Development Panel, jointly with the Climate Dynamics Panel, the Pacific Region Panel and other partners. On behalf of CLIVAR, I would like to thank the Japan Agency for Marine-Earth Science and Technology (JAMSTEC) for hosting the event, and to US CLIVAR and the Intergovernmental Oceanographic Commission (IOC) Sub-Commission for the Western Pacific (WESTPAC) for financial support to participants.

This is going to be a very important year for CLIVAR. All CLIVAR panels, the Scientific Steering Group (SSG) and the International CLIVAR Project Office (ICPO) are fully engaged in the organization of the CLIVAR Open Science Conference that will take place in a few months, on 18-25 September, in Qingdao, China. The success of the conference can already be shown by its numbers: 936 abstracts from 750 authors (66 countries) have been submitted and reviewed. Accepted contributions will be presented as orals or posters in 14 sessions. Twelve town halls will be organised that will provide a discussion forum for several communities. Jointly with the conference, CLIVAR, together with the Young Earth System Scientists (YESS) Community, is organising the Early Career Scientists Symposium (ECSS). For this event alone, we had 239 applicants, and 150 of those have been selected to attend the Symposium, based on the quality of their abstracts submitted to the OS. It will be a great opportunity for the future generation of climate scientists to not only learn more about CLIVAR activities, but also discuss and provide input on what they see as important climate science topics that CLIVAR should address. All of this in a friendly environment that will also allow them to network with colleagues from around the world. More details about the OSC and ECSS, including the latest programme, can be found at the conference website: www.clivar2016.org

In the Project Office, we had some recent staff changes. This is the first issue of Exchanges after I took over Anna Pirani's role as editor. Anna, who was an essential part of the ICPO since she joined in 2007, has taken on a new position as Head of the IPCC WG1 Technical Support Unit. Anna and her determination to improve CLIVAR as a whole will be missed, but I am sure we will continue to work together through CLIVAR's contribution to the IPCC process. I would like to wish every bit of success to Anna in her new role. And Jing Li has joined the ICPO team in Qingdao. Jing comes from the United Nations Development Programme (UNDP) in Beijing, where she has been Programme Assistant for Global Environmental Facility (GEF) Small Grants Programme (SGP) for over 6 years. Before that Jing worked at International Cooperation Department in State Oceanic Administration (SOA) of China for over 2 years, and worked as an Environmental Impact Assessment (EIA) Engineer for 1 years at the Third institute of oceanography/SOA, Xiamen, China. Jing is an environmentalist with a master degree in Environmental Science, specialized in Environmental Economics. Welcome Jing!

CLIVAR/JAMSTEC Workshop on the Kuroshio Current and Extension System: Theory, Observations, and Ocean Climate Modelling-The Workshop Overview and Outcomes

Yoshiki Komuro¹, Gokhan
Danabasoglu², Simon Marsland³,
Xiaopei Lin⁴, Shoshiro Minobe⁵, Anna
Pirani⁶, Tatsuo Suzuki¹, Ichiro Yasuda⁷

1. Japan Agency for Marine-Earth Science and Technology, Japan
2. National Center for Atmospheric Research, USA
3. CSIRO Oceans and Atmosphere, Australia
4. Physical Oceanography Laboratory/CIMSST, Ocean University of China and Qingdao National Laboratory for Marine Science and Technology, China
5. Hokkaido University, Japan
6. Université Paris Saclay, Saint-Aubin, France and The Abdus Salam International Centre for Theoretical Physics, Trieste, Italy
7. University of Tokyo, Japan

Introduction

The "CLIVAR/JAMSTEC Workshop on the Kuroshio Current and Extension System: Theory, Observations, and Ocean Climate Modelling" was held in Yokohama, Japan, January 12-13, 2016. The workshop was hosted by the Japan Agency for Marine-Earth Science and Technology (JAMSTEC), and jointly organized with three CLIVAR panels (Ocean Model Development Panel (OMDP), Pacific Regional Panel, and Climate Dynamics Panel) and the WESTPAC project on Air-Sea Interaction in the Kuroshio Extension and its Climate

Impact (AIKEC). International scientists contributed expertise of theoretical, observational, and numerical modelling studies of the Kuroshio. Seventy two participants from 9 countries presented 34 talks and 6 posters. Thanks to the NOAA Modeling, Analysis, Predictions and Projections (MAPP) Program, the workshop was live-streamed as a CLIVAR-NOAA webinar.

This CLIVAR Exchanges Special Issue highlights some of the topics presented and discussed at the workshop. Most of the presentations and abstracts, as well as more detailed information on the workshop, are available at: <http://www.clivar.org/omdp/kuroshio>

Workshop motivation and objectives

The Kuroshio, the western boundary current of the wind-driven gyre of the North Pacific Ocean, and the Kuroshio Extension (KE) current form a complex system along with other components in the western North Pacific. This system impacts on the local and global climate system in various ways. The Kuroshio transports a vast amount of heat from low to mid-latitudes, affecting both the global-scale energy balance and local climate. The KE and the recirculation gyre formed to the south of the Kuroshio act as a heat reservoir, penetrating through the atmospheric boundary layer as far as the upper troposphere. There is a strong meridional sea surface temperature (SST) gradient north of the KE, contributing to atmospheric storm activity. These significant impacts underline the importance of understanding the role of the KE on the climate and its variability.

For climate modelling to reproduce this complicated system we need ocean models with a horizontal resolution of at least about 20 km (eddy permitting), ideally 10 km or less (eddy resolving). Thanks to the enhancement of computational resources such models are now commonly applied to many related scientific topics. The "CLIVAR Working Group on Ocean Model Development (predecessor of OMDP) Workshop on High Resolution Ocean Climate Modelling" in 2014 highlighted many interesting studies with ocean models of 1/4° resolution or finer. Many climate modelling centres are planning to employ such high resolution ocean models in their contributions to the forthcoming Coupled Model Intercomparison Project Phase 6 (CMIP6). So it was most timely to share our experience and knowledge of theoretical, observational, and modelling studies, deepen our mutual understanding, and seek new collaborations during this workshop.

The objectives of the workshop were:

1. To assess the state-of-science of the theory, observations, and ocean climate modelling of the Kuroshio Current and Extension systems in the North Pacific Ocean;
2. To assess the role of higher resolution to improve the simulation of the Kuroshio system in ocean climate models;
3. To explore opportunities for new collaborative and focused studies on the Kuroshio Current and Extension system to improve decadal climate prediction capabilities both for the Asia-Pacific region and globally.

Keynote speakers

After short introductory remarks, the workshop began with two keynote presentations. Bo Qiu presented the KE decadal variability. A KE index (Qiu et al., 2014), calculated from four dynamical quantities related to the KE variability and representing stable/unstable phases of KE, was presented. The high correlation between the KE index and Pacific Decadal Oscillation (PDO) index shows that the large-scale KE variability is driven by basin-wide wind forcing. In addition,

non-linear oceanic eddy forcing is found to enhance the low-frequency variability in KE. This (decadal) KE variability affects the overlying storm-track activity as well as the regional sea level trends, mixed layer properties, and SST in the western North Pacific. The atmospheric response in turn enhances the KE decadal variations via oceanic feedbacks.

Ichiro Yasuda's presentation focused on the impact of KE variability on the marine ecosystem variability and climate. Significant inter-decadal variability has been observed in the catch of Japanese sardine, which lives in the KE region. The winter SST and mixed layer depth changes along the Kuroshio front have significant impacts on food availability for sardine larvae and subsequent survival of Japanese sardine. The Japanese sardine catch variability is coherent with northwestern U.S. climate variability that can be explained by the PDO's bi-decadal and penta-decadal components. The bi-decadal PDO component is closely related to the 18.6-yr period tidal oscillation through strong tidal mixing along the Kuril Straits. Surface and subsurface signals generated by this strong mixing propagate to the KE region and interact with the atmosphere.

Observation of the Kuroshio and KE

As one of the largest western boundary currents in the global ocean, the Kuroshio Current is an important and biologically productive system. Understanding the mechanisms of its variability helps to elucidate impacts on the marine ecosystem, ocean productivity, and climate change.

Meghan Cronin presented how data from the KE Observatory (KEO) surface mooring, combined with satellite SST data, are used to obtain the diffusivity values based on the mixed layer heat balance at KEO. By evaluating the budgets for both dissolved inorganic carbon and alkalinity from this estimated diffusivity, the export rate of both organic and inorganic carbon from the surface mixed layer can be distinguished and quantified, providing a baseline for the biological carbon pump in this dominant carbon sink region of the North Pacific Ocean.

Toshio Suga gave a review of the role of the KE in the ventilation of the North Pacific pycnocline. The wintertime mixed layers to both the south and north of the KE are among the deepest mixed layers in the North Pacific. Part of the large volume of water with properties renewed in this deep mixed layer spreads widely and ventilates a substantial part of the North Pacific pycnocline. The observed characteristics of this region as a ventilator of the pycnocline were reviewed.

Variability of the upstream region of the Kuroshio was presented by Kaoru Ichikawa. The variations of the position and speed of the Kuroshio axis were described. It is found that the Kuroshio current moves southward and its width becomes narrower when the axis speed is higher, and vice versa. Variations are revealed to be associated with anticyclonic (or cyclonic) offshore mesoscale eddies approaching from the east.

The interannual to decadal variability of KE was examined in Yoshinori Sasaki's presentation. Sea level variability along the Japanese coast is quite strong in the regions that are under the direct influence of jet-trapped Rossby waves, implying that the wind-driven circulation changes have significant impacts on the sea level variability in the KE region and along the coast of Japan.

Takeyoshi Nagai presented evidence of enhanced double-diffusive convection below the main stream of the KE. This research indicates that double-diffusive convection is enhanced by mesoscale subduction/obduction and near-

inertial motions, and thereby diapycnal tracer fluxes could be enhanced below the KE front.

Ocean Dynamics in the Kuroshio and KE, including multi-scale ocean processes

This session addressed notable ocean processes related to ocean and climate dynamics from various aspects: hot spots, surface wave mixing, water mass and front formation, ocean heat content variability, momentum balance of the KE, and regional sea level changes.

Xiaopei Lin highlighted the hot spots of the Kuroshio and KE. SST trends in the KE are affected by Kuroshio decadal variability driven by higher-latitude large-scale wind patterns. Multi-scale interaction is important to understand the Kuroshio variability. On behalf of Fangli Qiao, he explained that the mixing induced by non-breaking waves may add an important contribution to the vertical mixing process in the upper ocean. Using the climate model FIO-ESM with a parameterization of such mixing, the volume transport of Kuroshio in the East China Sea was realistically simulated.

Hideyuki Nakano addressed the formation of water masses in the northwestern Pacific. The Kuroshio-origin water is distributed in the subtropical gyre through Sverdrup circulation simulated using an eddy-resolving model including virtual tracers. There is a significant contribution from the marginal seas in the water mass distribution to the east of Japan.

Naoki Sato discussed the seasonal characteristics of the KE in early summer. Wind stress curl plays an important role in maintaining the meridional SST gradient along the KE through Ekman upwelling.

Bunmei Taguchi highlighted interannual to decadal ocean heat content variability in the North Pacific, addressing the generation and propagation processes of heat content anomalies. The eastward propagation occurs through anomalous spiciness advection and westward propagation via heaving of the thermocline. The spiciness signals are generated in the subarctic frontal zone near Japan.

Kunihiro Aoki discussed the Reynolds stress and interfacial form stress in the momentum equations to explain the downstream time mean decay of the KE jet. The eastward deceleration of the KE jet is governed by the ageostrophic Coriolis force and the meridional integral of the zonal Reynolds stress. The ageostrophic flow is partially driven by eddy kinetic energy (EKE). The relationship between the ageostrophic flow and EKE in the temporal mean may be explained by the mechanism of eddies accompanying curvature effect and migrating over the KE region.

Mio Terada reported on regional sea level change over the western North Pacific to the end of the 23rd century in CMIP5 models. The spatial patterns of regional sea level change evolve over the 21st, 22nd and 23rd centuries due to the intensification and the northward shift of the KE.

Development of ocean modelling: high-resolution modelling and reanalysis

This session explored impacts of bottom topography and resolutions of ocean models. Exciting developments exploring effects on climate and the Kuroshio of using high-resolution ocean models at regional to global scales were highlighted.

Masao Kurogi showed the effect of deep trenches and related bathymetry on the sea surface height field in the KE. Nested

high-resolution models are used, with resolutions of as high as 400-m, included barotropic and baroclinic dynamics, tracer advection, and sea-ice interactions. Simulations with a higher resolution nested ocean model — 100m resolution — are planned. Tsuyoshi Wakamatsu presented a 4D ocean data assimilation study of Kuroshio variability. The 1982-2014 reanalysis at 1/10° horizontal resolution was forced by JRA-55 reanalysis data. The Four-dimensional Variational Ocean ReAnalysis for the Western North Pacific (FORA-WNP30) product is available for research purposes at <http://synthesis.jamstec.go.jp/FORA/e/>, and is a recommended dataset for KE variability studies. It captures a series of stable/unstable periods, and offers insights into subsurface variability.

Helene Hewitt spoke on impacts of resolving/permitting mesoscale eddies in coupled climate simulations. A 1/12° global ocean model (NEMO) has been coupled to an N512 resolution atmosphere. Preliminary results indicate a 20% reduction in the Southern Ocean warm bias, a reduction in cold biases in the N. Hemisphere and some improvement in upwelling bias regions. Tides and shelf processes are resolved to study carbon uptake, marine impacts, and marine methane release.

Simona Masina explored KE decadal variability with a 1/4° horizontal resolution, 50-level version of NEMO, showing a large improvement from data assimilation over a free-running simulation with stable and unstable KE states reproduced in the former and not the latter. A new KE index that combines integrated wavelet amplitude and mean KE latitude is used to distinguish stable and unstable states of the KE.

Eric Chassignet presented a detailed study of the Gulf Stream separation, utilizing simulations with horizontal resolutions from 1/12° to 1/50°. The results were discussed in terms of power spectra with comparisons to the Kuroshio.

Air-sea interaction in the Kuroshio and KE and its climate impact

Presentations focused on air-sea heat fluxes, the atmospheric boundary layer, the free troposphere, and basin-scale atmospheric circulations.

Shoshiro Minobe introduced the newly formed CLIVAR Climate Dynamics Panel that fosters increased understanding of the dynamical processes that control circulation variability and change in the atmosphere and ocean on synoptic to centennial timescales. The focus of the Panel is on large-scale phenomena, processes, and mechanisms of coupled climate variability/modes, teleconnections and change on seasonal to centennial time-scales. At mid-latitudes, the ocean's influence on the atmosphere is especially strong along western boundary currents, such as the Kuroshio and the Gulf Stream, which provide heat and moisture to the atmosphere.

Studies of the mid-latitude ocean's influence on the atmosphere have rapidly developed in the last one and half decade, exploiting high-resolution observational data and numerical modelling. Atmospheric patterns coherent with oceanic structures, such as fronts and currents can be detected with high-resolution observational data analysis. Such studies indicate that oceanic forcing play an important role in the atmosphere given that scales of free-atmospheric variations are one order larger than oceanic ones. Using a new diagnostic for time-mean near-surface winds, Minobe showed different contributions of pressure adjustment and vertical mixing mechanisms; the former responsible for convergence/divergence of near-surface winds, while the latter for their rotation over the Gulf Stream, consistent with observational analysis using atmospheric temperatures observed by AIRS.

This strategy is referred to as a “scale-separation strategy”. An intrinsic limitation of this strategy exists when atmospheric responses occur on atmospheric spatial scales when studies must rely on numerical simulations.

Sergey Gulev presented air-sea heat fluxes associated with cyclones and anticyclones, showing that extremely large surface turbulent heat fluxes are associated with cyclone-anticyclone interaction zones, and that about 30% of cyclones propagating over the North Pacific provide more than 70% of the total turbulent heat loss.

Niklas Schneider presented the results of a simple atmospheric boundary layer model that resolves the two major mechanisms of the atmospheric responses in the boundary layer, i.e., the vertical mixing and pressure adjustment mechanisms. By exploiting linear dynamics, spectral solutions are obtained that are generally consistent with a high-resolution atmospheric model.

Hisashi Nakamura presented a new product of the Japanese Reanalysis (JRA-55HS) for which high-resolution SST is used – in contrast to the standard JRA-55 product with lower-resolution SSTs. The JRA-55HS is available for the 1985-2012 period, much longer than the ERA-interim high-resolution product. JRA-55HS is a legacy of the Japanese Hot-Spot project.

Using reanalysis data with high resolution SST, Ryusuke Masunaga showed differences in heat fluxes north of the KE for the stable and unstable regimes, and that high SST resolution in reanalysis products (JRA-55HS and ERA-interim after 2002) is important for reproducing important SST-induced atmospheric responses.

The importance of SST resolution is also shown in a numerical study by Justin Small with two versions of the Community Earth System Model (CESM): a high-resolution (nominal 0.1°) versus a low-resolution (nominal 1.0°) ocean model coupled with the same 0.25° atmospheric model. The study demonstrated that interannual variability of ocean-to-atmosphere surface turbulent heat fluxes are positively correlated with sea surface height in high-resolution CESM in mid-latitude frontal regions as observed, but this relationship is absent at low-resolution.

The local atmospheric response to SST fronts and eddies are well established. However, possible remote and large-scale atmospheric responses have much larger uncertainties. Ping Chang showed that ocean mesoscale eddies exert substantial impacts on the atmosphere even for basin-scale atmospheric circulations. The large-scale atmospheric influence of ocean eddies is a new finding, indicating the possible deficiency of IPCC-class climate models that do not resolve ocean eddies.

Akira Kuwano-Yoshida conducted two 20-year experiments with a 0.5° resolution atmospheric model; one with observed 0.25° SSTs and the other with smoothed SSTs in the Kuroshio and Oyashio regions. Rapidly deepening cyclones are more frequent in the control run than those in the smoothed run. The difference in the cyclone genesis results in basin-scale impacts on the atmospheric circulation and precipitation along the western coast of North America.

Stuart Bishop analyzed 100-year integrations of CESM with resolutions of 0.1° and 0.25° . The ocean and atmosphere meridional heat fluxes compensate each other through “Bjerknes Compensation” in winter over the North Pacific. Also, Shoshiro Minobe showed that the sharp SST front of the Gulf Stream is important to reproduce a realistic European blocking distribution and its associated cold-spells over Europe.

Several papers analyzed oceanic aspects of air-sea interactions. Tomoi Tozuka examined the mechanism by which the SST front of the KE is generated, using a heat budget in the mixed layer. Although heat flux from the ocean to the atmosphere is stronger south of the front, the weaker heat flux combined with the shallower mixed layer to the north of the front cools SSTs more efficiently there and thus produces a sharper SST front. Masami Nonaka studied the interaction between the tropics and mid-latitude North Pacific. Instead of the canonical El Niño, the El Niño Modoki caused a lagged response over the North Pacific, resulting in sea-surface height anomalies just to the south of the KE 3.5-year later. The influence of El Niño Modoki on the North Pacific is suggested to be enhanced in the last two decades. Hidenori Aiki showed air-sea momentum fluxes associated with oceanic surface waves in a regional air-sea coupled model significantly impact SST fields associated with tropical cyclones near Taiwan, suggesting that potential feedback from the ocean to tropical cyclones may be influenced with or without wave effect in the coupled model.

Marine ecosystems in the Kuroshio and KE

Hiroaki Saito presented an explanation of the “Kuroshio paradox” — how can the nutrient depleted Kuroshio sustain such diverse and abundant fish resources? Hapto-phyta is the dominant phytoplankton in the Kuroshio, which is different from other subtropical oligotrophic areas. The nutrient supply occurs through various processes: island and continental shelf sediments, riverine supply, turbulent mixing, and upwelling via front genesis. The food web is also different from nano-phytoplankton, here being predominantly gelatinous to doliolids planktons.

Keith Rodgers presented results from simulations using GFDL’s Earth system model ESM2M over the 1950-2100 period in comparison with phenomena observed along the 165°E JMA sections where decadal scale variability of subsurface pH and oxygen are observed during 1987-2012. This presentation pointed out that pH increasing trend at $26.6\sigma_\theta$ is more obvious than the trend of oxygen, suggesting that pH is more influenced by anthropogenic acidification. On the other hand, the subsurface oxygen variability is more influenced from natural variability propagated from upstream Central Mode Water.

Eitarou Oka showed the impact on the western boundary current regions from the formation of Subtropical Mode Water (STMW) whose formation rate changes with the decadal KE variability. After 2010, enhanced subduction of STMW was related to increased dissolved oxygen, pH, and aragonite saturation state. This coincided with decreased potential vorticity, apparent oxygen utilization, nitrate, and dissolved inorganic carbon. The changes of dissolved inorganic carbon, pH, and aragonite saturation state were opposite against their long-term trends. These results indicate a new mechanism consisting of westward sea surface height anomaly propagation, the KE state transition, and the STMW formation and subduction, by which the climate variability affects physical and biogeochemical structures in the ocean’s interior and potentially impacts the surface ocean acidification trend and biological production.

Workshop discussion and recommendations

There are several on-going and planned observational research programs around the KE region. We discussed objectives, research plans, and results of these programs: KEO surface mooring by NOAA-PMEL; a Japanese KEO observing project on the role of atmospheric dust in the marine biological pump; MEXT KAKENHI Innovative Study Ocean Mixing Processes: Impact on Biogeochemistry, Climate and Ecosystem (OMIX); and IOC-AIKEC. Overlaps and gaps among the projects were

examined, and the need and opportunities for future international collaborations among these parallel observational programs were vigorously discussed.

The KEO cruise will deploy 5000m deep sediment traps near the KEO buoy to understand the missing source of nutrients in ocean desert, in other words, the mechanisms of nutrient supply in oligotrophic NW Sub-tropical Pacific. The study will address how high primary production is supported or maintained in this region, the sources of nutrients of the ocean surface, the role of meso-scale eddies, meteorological events, eolian input, N₂ fixation and regeneration. Understanding these processes require observations over multiple years, yet funding for ship time must be applied for year by year. The workshop participants were extremely enthusiastic of these plans and sought to identify opportunities for collaboration. To better understand the upper ocean carbon flux, the cruise and sediment trap measurements could be combined with glider deployment. Integrating the results with satellite data would be very useful to interpret surface BGC and carbon flux.

The OMIX study will involve JMA annual CTC stations and vertical mixing measurements over next 4-5 years. Two gliders are planned to cross KE with microstructure measurements. Meghan Cronin encouraged OMIX to undertake validation measurements near the KEO buoy (CTD salinity measurements and water samples if possible).

IOC-AIKEC cruises are being undertaken by China yearly from 2014 to 2016. Moorings have been deployed near the KEO buoy as well as CTD sections and 20 Argo floats. The focus is on meso- and submeso-scale variability, inertial oscillations and areas of intense air sea exchange. In terms of long term plans, until 2020, an effort is underway to enhance international observation collaboration in the W. Pacific and E. Indian Ocean. 1 to 2 cruises are planned in this period in KE region to deploy and recover moorings. The cruises are open for participation and data exchange.

Results from the Japanese “Hot-Spot” extra-tropical air sea interaction study, which concluded in March 2015, is compiled in a special issue of *J. Oceanography* (October 2015). The NKEO buoy was deployed between KEO and J-KEO and access to all observational data including buoy data is open for the international community, following JAMSTEC regulations. This data is useful for model validation. Hope was expressed that Chinese studies will continue to collect data to build on the Hot Spot legacy.

Meghan Cronin concluded this discussion describing KEO, a component of the sustained observing system, as a magnet for process studies and deployments enabling research on processes, climate variability and change in the region. The community should envisage extending these capabilities to achieve a carbon ‘hot spot’ process study around KEO deploying new technologies, e.g. the saildrone—an unmanned sail boat, paired with underwater gliders. Observing small scale variability in air sea fluxes can be achieved by leveraging both Japanese and Chinese efforts, J-KEO and C-KEO respectively, including buoys north of the KE.

The discussion extended to the collaboration and synergy between observational and modelling studies. The Ocean Model Intercomparison Project (OMIP), which OMDP oversees as one of the endorsed MIPs in CMIP6, was introduced. Reliable observational data, preferably of long duration, is extremely important in order to evaluate model simulations. Reanalysis data also inherently depends on observations. On the other

hand, numerical models can provide fields with fine spatial/temporal resolution that cannot be obtained by observations. Regarding this viewpoint, it should be noted that some participants expressed their interest in JRA-55HS, a derivative of the Japanese reanalysis product JRA-55, that uses a high-resolution SST dataset (Nakamura et al., this issue).

An interesting discussion followed on the challenges of accessing observational data and the need for a “one-stop shopping site”. Several participants noted that it is difficult for many researchers to know where the observational data are, and what data are included in the reanalysis datasets. OceanSITES (<http://www.oceansites.org/>), part of the Global Ocean Observing System, is intended to be a one stop shop for modellers to obtain documented, formatted data and reference datasets for model development and testing. The response to the question “Where’s the Data” is provided by Meghan Cronin in this issue.

The need to constrain reanalysis products with observations was emphasized. WMO reference datasets should not be assimilated so they can be used to benchmark reanalysis products. The recommendation is that modelling centres do not assimilate reference data sets. If they are assimilated, it should be clearly stated to avoid redundancy in the validation of the reanalysis product. KEO sea level pressure has been assimilated into JRA55. However, temperature and other meteorological variables have not so these can be used to validate the JRA55 product.

Overall, the participants agreed to enhancing inter- and intra-observational and modelling coordination and collaboration. The workshop provided a great opportunity to share experience and knowledge, and promote future communication and collaboration among modelling/observational groups.



Figure : A group photo, at the entrance hall of JAMSTEC Yokohama Institute, January 13, 2016.

Acknowledgements

We, the scientific steering committee members, are grateful for sponsorship from Climate and Ocean – Variability, Predictability, and Change (CLIVAR), US CLIVAR, Japan Agency for Marine-Earth Science and Technology (JAMSTEC), and Intergovernmental Oceanographic Commission (IOC). This workshop was also supported by MEXT Grant-in-Aid for Scientific Research on Innovative Areas Number H05825. We are also grateful to the NOAA Modeling, Analysis, Predictions and Projections (MAPP) Program for their generous support in live streaming the workshop. We would like to thank Prof. Bo Qiu for organizing a discussion session in the workshop and providing valuable comments for this article. Thanks are extended to the local administrative staff, the oral and poster presenters, and all the participants for their contributions that made the workshop a great success.

References

- Cronin, M. F., 2016: Where's the Data? CLIVAR Exchanges 69 [this issue]
- Nakamura H., Y. Kawai, R. Masunaga, H. Kamahori, C. Kobayashi, and M. Koike, 2016: An extra product of the JRA-55 atmospheric reanalysis and in-situ observations in the Kuroshio-Oyashio Extension under the Japanese "Hotspot project." CLIVAR Exchanges 69 [this issue]
- Qiu, B., S. Chen, N. Schneider, and B. Taguchi, 2014: A coupled decadal prediction of the dynamic state of the Kuroshio Extension system. *J. Climate*, 27, 1751-1764.

Inter-Decadal Modulations in the Dynamical State of the Kuroshio Extension System: 1905-2015

Bo Qiu, Shuiming Chen, and Niklas Schneider

Department of Oceanography, University of Hawaii at Manoa

Introduction

After separating from the Japanese coast at 36°N, 141°E, the Kuroshio enters the open basin of the North Pacific, where it is renamed the Kuroshio Extension (KE). Free from the constraint of coastal boundaries, the KE has been observed to be an eastward-flowing inertial jet accompanied by large-amplitude meanders and energetic pinched-off eddies (see, e.g., Qiu, 2002a for a comprehensive review). Compared to its upstream counterpart south of Japan, the KE is accompanied by a stronger southern recirculation gyre (RG) that increases the KE's eastward volume transport to more than twice the maximum Sverdrup transport (~60Sv) in the subtropical North Pacific Ocean, enhancing its nonlinear nature as a western boundary current extension. In addition to the high level of mesoscale eddy variability, an important feature emerging from recent satellite altimeter measurements and eddy-resolving ocean model simulations, is that the KE system exhibits clearly-defined decadal modulations between a stable and an unstable dynamic state (e.g., Qiu, 2003; Qiu & Chen, 2005, 2010; Taguchi et al., 2007, 2010; Cebollas et al. 2009; Sugimoto and Hanawa, 2009; Kelly et al. 2010; Sasaki et al., 2013). As shown on the cover page of this Exchanges issue, the KE paths were relatively stable in 1993–1995, 2002–2005 and 2010–2015. In contrast, spatially convoluted paths prevailed during 1996–2001 and 2006–2009. It is important to emphasize that these changes in path stability are merely one manifestation of the decadal-modulating KE system. When the KE jet is in a stable dynamic state, available satellite altimeter data further reveal that its eastward transport and latitudinal position tend to be greater and more northerly, its southern RG tends to strengthen, and the regional eddy kinetic energy level tends to decrease. The reverse is true when the KE jet switches to an unstable dynamic state.

KE index during the satellite era

To succinctly summarize the time-varying dynamical state of the KE system, Qiu et al. (2014) introduced the KE index defined as average of the variance-normalized time series of

the southern RG intensity, the KE's intensity, its latitudinal position, and negative of its path length. A positive KE index, thus defined, indicates a stable dynamical state and a negative KE index, an unstable dynamical state. The red line in Figure 1c shows the KE index in the satellite altimetry period of 1993–2015. Dominance of the decadal modulation in the KE system is easily discernible in this time series. Transitions between the KE's two dynamical states are caused by the basin-scale wind stress curl forcing in the eastern North Pacific related to the Pacific decadal oscillations (PDOs). Specifically, when the central North Pacific wind stress curl anomalies are positive (i.e. positive PDO phase), enhanced Ekman flux divergence generates negative local sea surface height (SSH) anomalies in 170°–150°W along the southern RG latitude (see Figures 1a and 1b). As these wind-induced negative SSH anomalies propagate westward as baroclinic Rossby waves into the KE region after a delay of 3–4 years, they weaken the zonal KE jet, leading to an unstable (i.e., negative index) state, of the KE system with a reduced recirculation gyre and an active eddy kinetic energy field. The negative, anomalous wind stress curl forcing during the negative PDO phase, on the other hand, generates positive SSH anomalies through the Ekman flux convergence in the eastern North Pacific. After propagating into the KE region in the west, these anomalies stabilize the KE system by increasing the KE transport and by shifting its position northward, leading to a positive index state.

A regression analysis in Qiu et al. (2014) reveals that the KE index defined by the 4 dynamical properties can be favourably represented by the sea surface height (SSH) signals inside the KE's southern RG region of 31°–36°N and 140°–165°E (black lines in Figure 1c). The linear correlation coefficient between the red and thick (thin) black lines in Figure 1c is as high as 0.97 (0.84). Physically, this high correlation is of little surprise because the large-scale KE variability is closely entwined to the dynamical state of its southern RG and the RG's variability is well represented by its regional SSH signals. On a practical level, this makes exploration of the KE dynamical state be equivalent to examination of the SSH signals in the key region of the KE's southern RG.

As evidenced in Figure 1b, changes in the mid-latitude wind-forced SSH field is governed by westward-propagating Rossby wave adjustment processes (see Qiu, 2002b, and references therein, for theoretical justification). Figure 1d shows the SSH time series averaged in the 31°–36°N and 140°–165°E box based on the 1.5-layer reduced-gravity model forced by the monthly ECMWF ERA-Interim wind stress data (Dee et al., 2014). The correlation between this modelled SSH time series and that shown in Figure 1c (thick black line) reaches 0.85, demonstrating the usefulness of the wind-forced 1.5-layer reduced-gravity model in capturing the decadal modulations of the KE dynamical state during the past quarter of a century.

KE index over the past century

Use of the SSH signals in the southern RG box as a proxy for the KE dynamical state allows us to explore the KE index variations beyond the satellite altimetry era. To achieve this, we merge the ECMWF reanalysis wind stress product ERA-20C (available from 1900 to 2010; Stickler et al., 2014) and ERA-Interim (available from 1979 to 2015) and force the 1.5-layer reduced-gravity model (over the overlapping period of 1979–2010, the merge is done bi-linearly). Figure 2a shows the model-derived SSH changes in the KE's southern RG box of 31°–36°N and 140°–165°E. Notice that to focus on the decadal variability, we have removed the long-term increasing linear trend of 1.5 cm/decade from Figure 2a; also, no SSH signals are evaluated in the first 5 years due to the model spin-up. For comparison and serving as an independent check, we plot in Figure 2b the time series of surface dynamic height calculated from the historical, objectively-analyzed, T/S data compiled by Ishii et al. (2006) in the same southern RG box from 1945 to 2012. Because the available T/S data is confined to the upper ocean of 1,500m, the amplitude of the T/S-based KE index is, on average, about half that derived from the wind-forced 1.5-layer reduced-gravity model. However, the observed phase changes of the KE index agree well with those predicted by the wind-forced model hindcast. Note that the agreement between Figures 2a and 2b improves after 1960s when the in-situ T/S measurements became more abundant: the linear correlation coefficient between the two time series in 1960–2012 is 0.82, as compared to 0.74 during the overlapping period of 1945–2012.

Both Figures 2a and 2b reveal that the low-frequency modulation of the KE dynamical state is not confined to the last two decades during which we had satellite-based SSH information to capture the detailed evolution of the KE system. To examine how the dominant period of the century-long KE index has modulated over the past century, we plot in Figure 2c the wavelet power spectrum for the KE index time series shown in Figure 2a. Large-amplitude decadal changes can be seen to persist after the mid-1970s. From mid-1940s to mid-1970s, the KE index appears to have two dominant periods: one in the 15–20-year band and the other in the 4–6-year band. Note that the short 4–6-year variability in the KE index

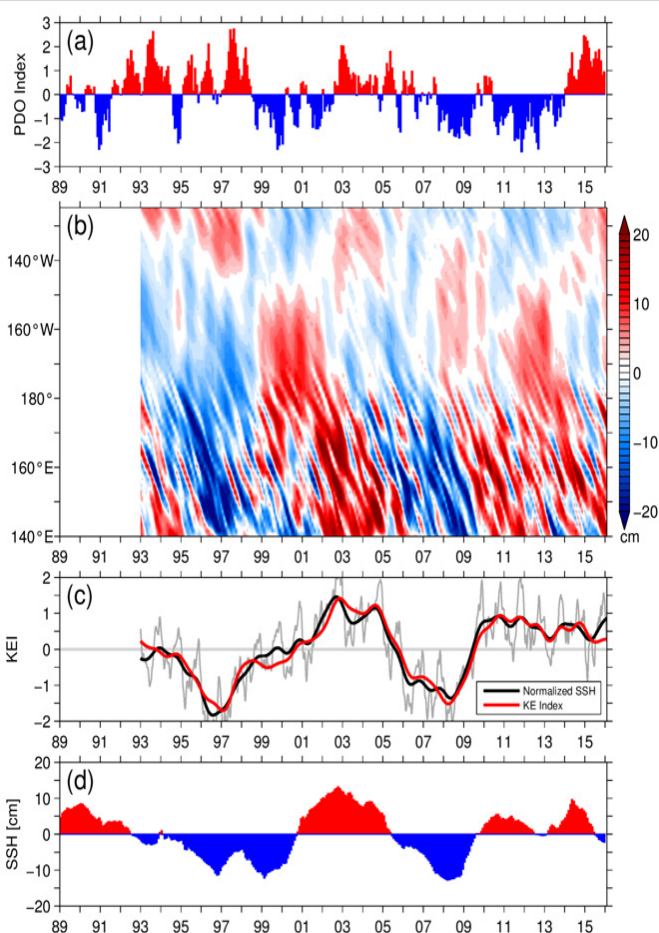


Figure 1: (a) Time series of Pacific decadal oscillation (PDO) from <http://jisao.washington.edu/pdo/PDO.latest>. (b) SSH anomalies along the zonal band of 32°–34°N from the AVISO satellite altimeter data. (c) Time series of the KE index synthesized from four dynamical properties (red line) versus the normalized SSH anomalies averaged in 31°–36°N and 140°–165°E (black lines); here, the thin black line denotes the weekly time series and the thick black line the low-pass filtered time series. (d) SSH anomalies in the 31°–36°N and 140°–165°E box predicted by the 1.5-layer reduced-gravity model forced by the ECMWF Interim wind stress data.

was also detected in the eddy-resolving OFES model output of 1955–1975 that was forced by the NCEP-NCAR reanalysis wind stress data (Qiu et al., 2014; their Figure 5a). In between the mid-1920s and mid-1940s, the KE index appears to be dominated by the 10–15-year fluctuations and prior to the mid-1920s, Figure 2c indicates that the predominant period

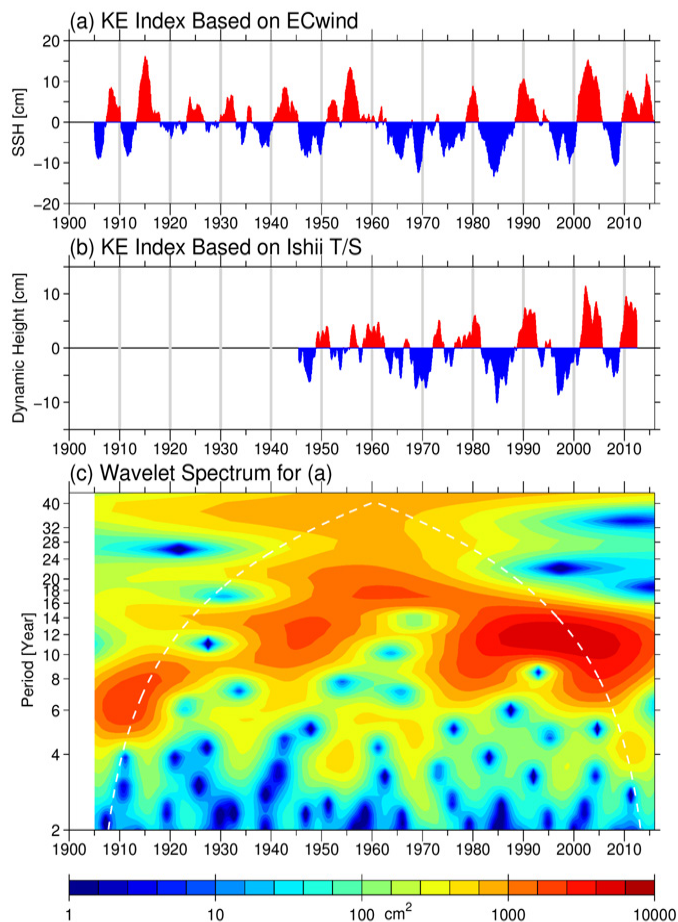


Figure 2: (a) KE index time series based on the SSH anomalies in the 31°–36°N and 140°–165°E box predicted by the 1.5-layer reduced-gravity model forced by the merged ERA-20C and Interim wind stress data. (b) KE index time series based on the SSH anomalies in the 31°–36°N and 140°–165°E box calculated from the historical T/S data of Ishii et al. (2006). Notice the difference from (a) in y-axis scale. (c) Wavelet power spectrum for the time series of (a).

of the time-varying KE index falls in between 6 and 10 years.

It is worth emphasizing that the mid-1920s, mid-1940s, and mid-1970s marked the three 20th-century climatic regime shifts in the Aleutian Low pressure system over the North Pacific Ocean (e.g., Minobe, 1997; Zhang et al., 1997). The results in Figure 2 clearly indicate that these regime shifts in the atmospheric forcing field exert a significant impact upon the frequency content of the time-varying KE system. What is yet to be explored and quantified is the degree to which the variability in the KE dynamical state may feedback to the low-frequency changes in the overlying atmospheric circulation. By transporting warmer tropical water to the mid-latitude ocean, the expansive KE provides a significant source of heat and moisture for the North Pacific mid-latitude atmospheric storm tracks (e.g., Nakamura et al., 2004). By modifying the path and intensity of the wintertime overlying storm tracks, changes in the KE dynamic state can alter not only the stability and pressure gradient within the local atmospheric boundary layer, but also the basin-scale wind stress pattern (Taguchi et al., 2009; Kwon et al., 2010; Frankignoul et al., 2011; Kwon and Joyce, 2013). After the latest regime shift of the mid-1970s, Qiu et al. (2007; 2014) show that a positive (negative) index

KE state tends to generate a positive (negative) wind stress curl in the eastern North Pacific basin, resulting in negative (positive) local SSH anomalies through Ekman divergence (convergence). This impact on wind stress induces a delayed negative feedback with a preferred period of ~10 years and is likely the cause for the enhanced decadal variance demonstrated in Figure 2. It will be important for future studies to clarify if similar feedback mechanisms are at work within the epochs of other climatic regime shifts in the 20th century.

Acknowledgments

The ERA-Interim and ERA-20C surface wind stress data are provided by ECMWF and the merged satellite altimeter data by the Copernicus Marine and Environment Monitoring Service (CMEMS). Support from NASA NNX13AE51G and NSF OCE-0926594 is acknowledged.

References

- Ceballos, L., E. Di Lorenzo, C. D. Hoyos, N. Schneider, and B. Taguchi, 2009: North Pacific Gyre oscillation synchronizes climate variability in the eastern and western boundary current systems. *J. Climate*, 22, 5163–5174.
- Dee, D. P., M. Balsameda, G. Balsamo, R. Engelen, A. J. Simmons, and J.-N. Thépaut, 2014: Toward a Consistent Reanalysis of the Climate System. *Bull. Amer. Meteor. Soc.*, 95, 1235–1248.
- Frankignoul, C., and N. Sennéchaël, Y.-O. Kwon, and M.A. Alexander, 2011: Influence of the meridional shifts of the Kuroshio and the Oyashio Extensions on the atmospheric circulation. *J. Climate*, 24, 762–777.
- Kelly, K.A., R.J. Small, R.M. Samelson, B. Qiu, T.M. Joyce, Y.-O. Kwon and M.F. Cronin, 2010: Western boundary currents and frontal air-sea interaction: Gulf Stream and Kuroshio Extension. *J. Climate*, 23, 5644–5667.
- Kwon, Y.-O., and T.M. Joyce, 2013: Northern hemisphere winter atmospheric transient eddy heat fluxes and the Gulf Stream and Kuroshio-Oyashio Extension variability. *J. Climate*, 26, 9839–9859.
- Kwon, Y.-O., M. A. Alenxader, N. A. Bond, C. Frankignoul, H. Nakamura, B. Qiu, and L. Thompson, 2010: Role of the Gulf Stream and Kuroshio-Oyashio Systems in large-scale atmosphere-ocean interaction: A review. *J. Climate*, 23, 3249–3281.
- Ishii, M., M. Kimoto, K. Sakamoto, and S.-I. Iwasaki, 2006: Steric sea level changes estimated from historical ocean subsurface temperature and salinity analyses. *J. Oceanogr.*, 62, 155–170.
- Minobe, S., 1997: A 50–70 year climatic oscillation over the North Pacific and North America. *Geophys. Res. Lett.*, 24, 683–686.
- Nakamura, H., T. Sampe, Y. Tanimoto, and A. Shimpo, 2004: Observed associations among storm tracks, jet streams and midlatitude oceanic fronts. *Earth's Climate: The Ocean-Atmosphere Interaction*, Geophys. Monogr., 147, Amer. Geophys. Union, 329–346.
- Qiu, B., 2002a: The Kuroshio Extension system: Its large-scale variability and role in the midlatitude ocean-atmosphere interaction. *J. Oceanogr.*, 58, 57–75.
- Qiu, B., 2002b: Large-scale variability in the midlatitude

subtropical and subpolar North Pacific Ocean: Observations and causes. *J. Phys. Oceanogr.*, 32, 353-375.

Qiu, B., 2003: Kuroshio Extension variability and forcing of the Pacific decadal oscillations: Responses and potential feedback. *J. Phys. Oceanogr.*, 33, 2465-2482.

Qiu, B., and S. Chen, 2005: Variability of the Kuroshio Extension jet, recirculation gyre and mesoscale eddies on decadal timescales. *J. Phys. Oceanogr.*, 35, 2090-2103.

Qiu, B., and S. Chen, 2010: Eddy-mean flow interaction in the decadal modulating Kuroshio Extension system. *Deep-Sea Res. II*, 57, 1098-1110.

Qiu, B., N. Schneider, and S. Chen, 2007: Coupled decadal variability in the North Pacific: An observationally-constrained idealized model. *J. Climate*, 20, 3602-3620.

Qiu, B., S. Chen, N. Schneider, and B. Taguchi, 2014: A coupled decadal prediction of the dynamic state of the Kuroshio Extension system. *J. Climate*, 27, 1751-1764.

Sasaki, Y. N., S. Minobe and N. Schneider, 2013: Decadal response of the Kuroshio Extension jet to Rossby waves: Observation and thin-jet theory. *J. Phys. Oceanogr.*, 43, 442-456.

Stickler, A., S. Brönnimann, M. A. Valente, J. Bethke, A. Sterin, S. Jourdain, E. Roucaute, M. V. Vasquez, D. A. Reyes, R. Allan, and D. Dee, 2014: ERA-CLIM: Historical Surface and Upper-Air Data for Future Reanalyses. *Bull. Amer. Meteor. Soc.*, 95, 1419-1430.

Sugimoto, S., and K. Hanawa, 2009: Decadal and interdecadal variations of the Aleutian Low activity and their relation to upper oceanic variations over the North Pacific. *J. Meteor. Soc. Japan*, 87, 601-614.

Taguchi, B., H. Nakamura, M. Nonaka, and S.P. Xie, 2009: Influences of the Kuroshio/Oyashio Extensions on air-sea heat exchanges and storm-track activity as revealed in regional atmospheric model simulations for the 2003/04 cold season. *J. Climate*, 22, 6536-6560.

Taguchi, B., S.-P. Xie, N. Schneider, M. Nonaka, H. Sasaki, and Y. Sasai, 2007: Decadal variability of the Kuroshio Extension. Observations and an eddy-resolving model hindcast. *J. Climate*, 20, 2357-2377.

Taguchi, B., B. Qiu, M. Nonaka, H. Sasaki, S.-P. Xie, and N. Schneider, 2010: Decadal variability of the Kuroshio Extension: mesoscale eddies and recirculations. *Ocean Dyn.*, 60, 673-691.

Zhang, Y., J. M. Wallace, and D. S. Battisti, 1997: ENSO-like Interdecadal Variability: 1900–93. *J. Climate*, 10, 1004-1020.

Variability and Mixing in the Kuroshio and Impact on Ecosystem and Climate

Ichiro Yasuda

Atmosphere and Ocean Research Institute, The University of Tokyo, Japan

Introduction

Decadal to inter-decadal variability of the Kuroshio and the Kuroshio Extension has a tremendous impact on ecosystem and fisheries around Japan. One example is the Japanese sardine (*Sardinops melanostictus*) which showed drastic variability in the last three centuries (e.g. Yasuda et al., 1999). The main causes of the Kuroshio Current system variability and thus the Japanese sardine have been attributed to the basin-scale North Pacific variability such as Pacific Decadal Oscillation (PDO, Mantua et al., 1997). PDO has two dominant inter-decadal components, bi-decadal and penta-decadal variability; the latter penta-decadal period is 3 times the bi-decadal one, and these two components change signs nearly simultaneously to cause remarkable regime shifts (Minobe, 1999; Minobe and Jin, 2004). Although reasons that determines the timescale of the bi-decadal and penta-decadal period variability are not been yet known, one possibility is the 18.6-year lunar tidal cycle and the resulting vertical mixing variability in the ocean (e.g. Loder and Garrett, 1978), which could connect all the variability. This report reviews the recent studies on sardine variability and 18.6-year period tidal cycle, and introduces a Japanese 5-year project "Ocean Mixing Processes: Impact on Biogeochemistry, Climate and Ecosystem (OMIX)".

Japanese sardine variability

In the 20th century, catch of the Japanese sardine had two peaks in the 1930s and 1980s. Sardine catches started to increase in the early 1970s, peaked in 1988 (it reached over 4.5 million tons which corresponds to over 1/3 of Japanese total catch and 1/20 of the world total), and has declined since 1989. The decline is credited to the continuous very low survival rates of 1988-1991 year classes and subsequent low rates in the 1990s (Watanabe et al., 1995 and subsequent data from Japan Fisheries Research Agency). Year-to-year survival rate variability during 1979-1994 was found to be negatively correlated with January-April sea surface temperature (SST) (Noto and Yasuda, 1999; 2003) and winter mixed layer depth (MLD) (Nishikawa and Yasuda, 2008) in the area south of the Kuroshio Extension (30-35°N, 145°-180°E) whose winter-spring warm (cold) and shallow (deep) winter mixed layer well corresponds to the low (high) survival rates during 1988-1991 (1979-1987). Further detailed studies using high resolution hindcast modelling showed that SST and MLD variability south of the Kuroshio Extension correspond well to winter SST and MLD variability along the Kuroshio main stream (Nishikawa and Yasuda, 2011) where sardine larvae are transported to

the Kuroshio Extension (Nishikawa et al., 2011; 2013a; Itoh et al., 2009; 2011), especially along the northern side of the stream axis. In this region winter deep ML and winter-spring low SST could cause high survival through nutrient supply during winter and subsequent enhanced spring plankton bloom and appropriate temperature environment (Nishikawa et al., 2013a; 2013b). In the frontal zone on the northern side of the Kuroshio axis, vertical mixing and nitrate diffusive flux are significantly enhanced (Kaneko et al., 2012; 2013), and could maintain the high biological production zone just north of the Kuroshio Extension Front even after spring bloom, when sardine larvae are transported and enhanced vertical mixing increases the productivity (Nishikawa et al., 2013b). The decadal winter SST and MLD variability are caused by variations in the Kuroshio current speed (Fig. 1b) due to: i) the arrival of westward propagating baroclinic Rossby waves excited by Aleutian Low variability, and ii) atmospheric cooling variability; The relative contribution of i) and ii) is 2:1 to SST/MLD variability (Nishikawa and Yasuda, 2011).

PDO and 18.6-year lunar cycle

PDO consists of co-variability of mid-latitude SST and sea level pressure (SLP) of Aleutian Low Pressure system. The SST and SLP difference between the strong and weak diurnal tides in the 18.6-year cycle is similar to the negative PDO pattern (Fig. 2a, modified from Fig. 1 of Yasuda et al. 2006); the Aleutian Low pressure is weak and positive SST anomalies (SSTa) east of Japan and in the central North Pacific and negative SSTa along the west coast of North America. The 18.6-year period lunar tidal cycle is caused by the variation of inclination of moon orbital plane to the earth equatorial plane from 18.4° to 28.4°. In the former, semi-diurnal (diurnal) tide is strong (weak), and the opposite is true in the latter. The amplitude modulation rates of diurnal (semi-diurnal) tidal forces change by 19% in O_1 and 11% in K_1 (4% in M_2 and 30% in K_2) to each mean amplitude.

The diurnal tides in the Kuril Straits are quite strong due to the resonance between the diurnal tidal forcing and diurnal topographically trapped internal tidal waves around Kuril Islands. The very cold (2°C) subsurface water upwells due to strong tide-induced turbulent vertical mixing as shown in Fig. 2c (Itoh et al., 2010; 2011; 2014; Yagi and Yasuda, 2012; 2013; Ono et al., 2013; Yagi et al., 2014; Tanaka et al., 2014). This enhanced turbulence changes by up to 20% in the 18.6-year tidal cycle, and was hypothesized to lead to the bi-decadal ocean and climate variability (Yasuda et al., 2006). In fact, in the downstream regions of the enhanced diurnal tides through the Kuril Straits and Aleutian Passes, surface to intermediate depths bi-decadal variability have been demonstrated on several variables: surface salinity, intermediate-depth isopycnal oxygen, temperature, salinity and thickness in the Oyashio and the Okhotsk Sea (Osafune and Yasuda, 2006) and eastern Bering Sea (Osafune and Yasuda, 2010; 2012), and phosphate in the Oyashio and east of Japan (Tadokoro et al., 2009). Numerical modelling results of this variability were shown by Osafune and Yasuda (2012; 2013).

The 18.6-year cycle is also seen in the climate indices such as winter North Pacific Index (Aleutian Low Pressure), winter East-Asian Monsoon Index and PDO (Yasuda et al., 2006). 18.6-year spectrum peak is significantly detected in the 270 year-long record of PDO reconstructed from tree rings (Fig. 2b), and the phase is found to be locked to the 18.6-year cycle (negative (positive)-PDO in the 3rd to 5th (9th to 12th) year from maximum diurnal tide (Yasuda, 2009). A climate model experiment with enhanced vertical mixing around the Kuril Straits suggested that the impact propagates as coastal and equatorial waves and affects the ENSO and PDO (Hasumi et al., 2008). Another climate model experiment with parameterized internal tidal mixing and 18.6-yr variation in the global oceans yielded the similar observed co-variability of SST and SLP of PDO and suggested the importance of Kuril tidal mixing variability, which is amplified by air-sea interaction between SST anomalies in the Kuroshio-Oyashio Extension regions and the Aleutian Low (Tanaka et al., 2012). Although these climate models reproduced some key observational features, important features such as time-lag, baroclinic waves and tropical/equatorial bi-decadal variability have not been sufficiently reproduced, probably because of unknown vertical mixing processes and distributions and of insufficient mixing parameterization.

Future studies and OMIX

As stated above, many issues come from vertical mixing, which is the most under sampled physical property in the oceans and changes by order of 4 in space and time. This large variability and its 18.6-year modulation could have tremendous impacts on ocean circulation, biogeochemistry, climate and ocean ecosystem/fisheries.

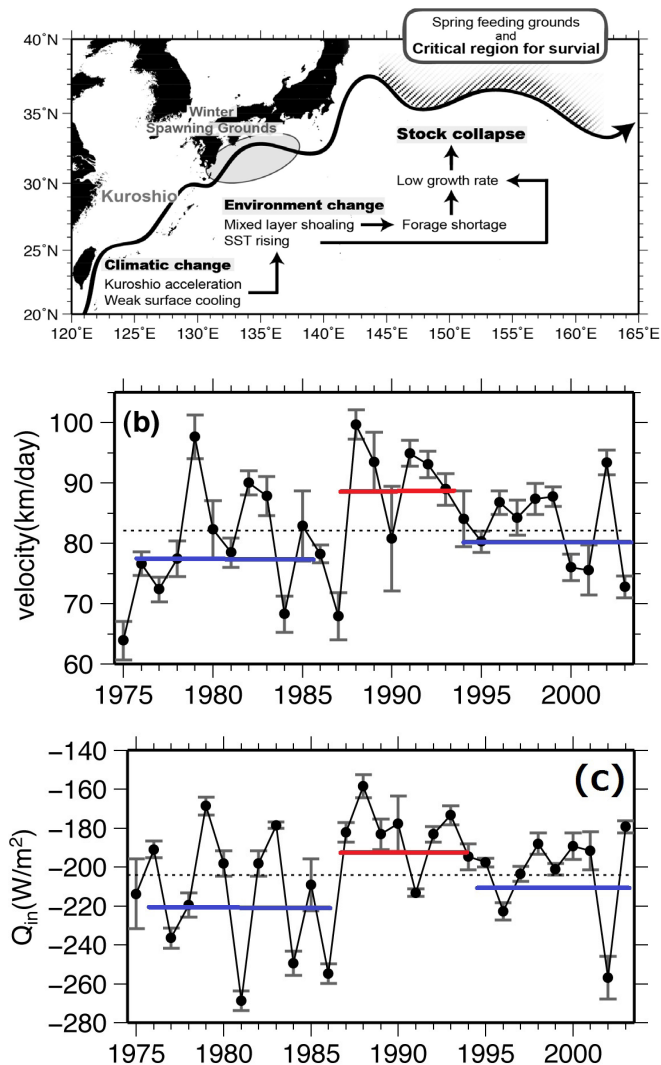


Figure 1: (a) Schematic representation showing the relationship between Japanese sardine and the Kuroshio decadal-scale variability (modified from Fig. 12 of Nishikawa et al., 2013b). Intensification (weakening) of the Kuroshio velocity (b) (modified from Fig. 14b of Nishikawa and Yasuda 2011) as well as weakened (intensified) winter cooling (c) correspond to warm (cold) and shallow (deep) winter mixed layer denoted by red (blue) horizontal bars (modified from Fig. 12b of Nishikawa and Yasuda 2011). Sardines spawned south of Japan in winter are transported along the Kuroshio where sardine larvae are better survived in the environment of colder and deeper mixed layer with higher nutrients which lead to greater and longer-lasting spring bloom because of the enhanced vertical mixing along the northern side of the Kuroshio.

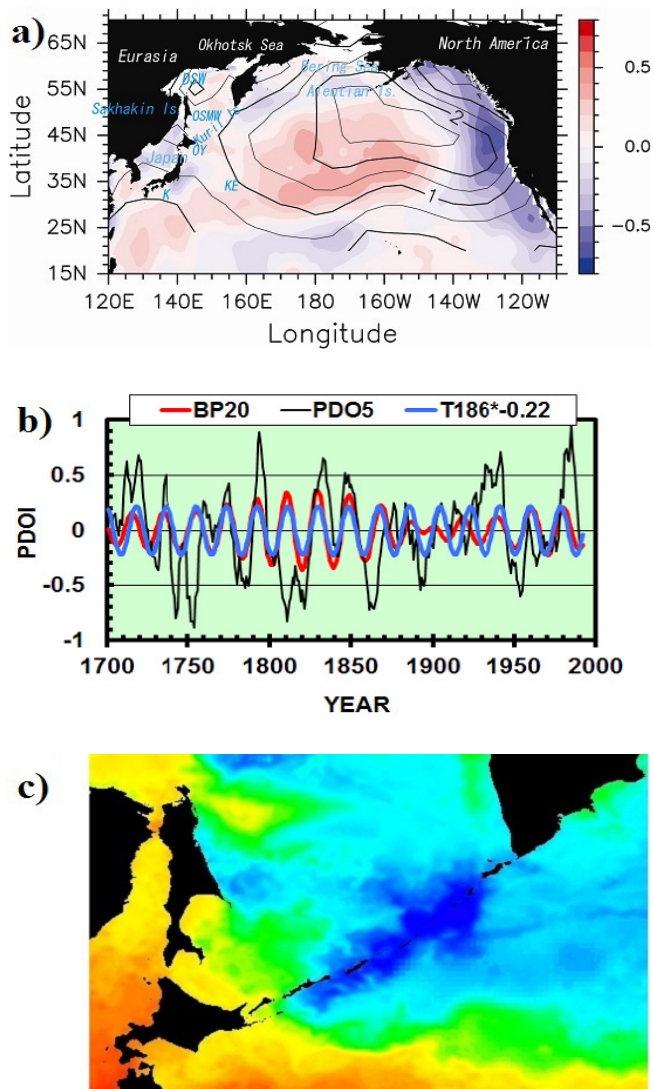


Figure 2: (a) Difference of SST (color shade in °C), SLP (contours in hPa) and wind direction (arrows) between the periods of strong and weak diurnal tide in the 18.6-year period tidal cycle (modified from Fig. 1 of Yasuda et al., 2006). (b) Time-series of 5-year running mean Pacific Decadal Oscillation (PDO) index (black) reconstructed from tree-rings, 15.5-23.3-year bandpass (red) and inverted-18.6-year tidal cycle (blue) (modified from Fig. 2 of Yasuda, 2009). (c) Satellite SST on July 28 in 2006 showing the cold SST around the Kuril Straits due to strong diurnal tidal mixing where the dark blue color denoting about 2°C. Orange color denotes about 20°C. Observations and climate model experiments suggest that 18.6-year mixing variability around the Kuril Straits regulates and yields the rhythm for the bi-decadal ocean and climate variability such as PDO.

Vertical mixing could modify the deep and intermediate ocean circulation. Enhanced vertical mixing in the western Pacific and east-Asian marginal seas with relatively large internal tides, strong western boundary currents and rough topography could cause enhanced nutrient supply and biological production. These could sustain the world largest biological uptake of carbon dioxide (Takahashi et al., 2002) and abundant fisheries with 26% landings in only 6% sea surface area. The enhanced vertical mixing upwells iron to the surface, and could control the biological production in the western subarctic high nutrient, low chlorophyll (HNLC) areas (Nishioka et al., 2013) and in the Green Belt along the continental slope of the eastern Bering Sea (Tanaka et al., 2012; 2013; 2015). Bi-decadal and its 3 times long penta-decadal ocean and climate variability could be explained by 18.6-year tidal cycle and its related variability. Over 60 researchers launched a 5-year project OMIX in July

2015, to test hypotheses and resolve issues mentioned above, by performing integrated observations and by developing numerical models with vertical mixing processes. OMIX welcomes international collaborators, with more information available on the project website: <http://omix.aori.u-tokyo.ac.jp/en/>.

References

- Hasumi, H., I. Yasuda and H. Tatebe, M. Kimoto, 2008: Pacific bi-decadal variability regulated by tidal mixing around the Kuril Islands. *Geophys. Res. Lett.*, 35, L14601, doi:10.1029/2008GL034406.
- Itoh, S., I. Yasuda, H. Nishikawa, H. Sasaki and Y. Sasai, 2009: Transport and environmental temperature variability of eggs and larvae of the Japanese anchovy (*Engraulis japonicus*) and Japanese sardine (*Sardinops melanostictus*) in the western North Pacific estimated via numerical particle tracking experiments. *Fish. Oceanogr.*, 18(2), 118-133.
- Itoh, S., I. Yasuda, T. Nakatsuka J. Nishioka, and Y. N. Volkov, 2010: Fine- and microstructure observations in the Urup Strait, Kuril Islands, during August of 2006. *J. Geophys. Res. Oceans*, 115, C08004, doi:10.1029/2009JC005629
- Itoh, S., T. Saruwatari, H. Nishikawa, I. Yasuda, K. Komatsu, A. Tsuda, T. Setou, and M. Shimizu, 2011: Environmental variability and growth histories of larval Japanese sardine (*Sardinops melanostictus*) and Japanese anchovy (*Engraulis japonicus*) near the frontal area of the Kuroshio. *Fish. Oceanogr.*, 20(2), 114-124.
- Itoh, S., I. Yasuda, M. Yagi, H. Kaneko, S. Osafune, T. Nakatsuka J. Nishioka, and Y. N. Volkov, 2011: Strong vertical mixing in the Urup Strait. *Geophys. Res. Letters*, VOL. 38, L16607, doi:10.1029/2011GL048507.
- Itoh, S., Y. Tanaka, S. Osafune, I. Yasuda, M. Yagi, H. Kaneko, S. Konda, J. Nishioka and Y.N. Volkov, 2014: Direct breaking of large-amplitude internal waves in the Urup Strait. *Progress in Oceanography*, 126, 109-120.
- Kaneko, H., I. Yasuda, K. Komatsu, and S. Itoh, 2012: Observations of the structure of turbulent mixing across the Kuroshio. *Geophys. Res. Lett.*, 39, L15602, doi:10.1029/2012GL052419.
- Kaneko, H., I. Yasuda, K. Komatsu, and S. Itoh, 2013: Structure of vertical nitrate flux across the Kuroshio jet. *Geophys. Res. Letters*, 40, 3123-3127.
- Loder, J. W., and C. Garrett, 1978: The 18.6-year cycle of sea surface temperature in shallow seas due to variation in tidal mixing. *J. Geophys. Res.*, 83, 1967-1970.
- Mantua, N. J., S. R. Hare, Y. Zhang, J. M. Wallace, and R. C. Francis, 1997: A Pacific interdecadal climate oscillation with impacts on salmon production. *Bull. Am. Meteorol. Soc.*, 78, 1069-1079.
- Minobe, S., 1999: Resonance in bi-decadal and pentadecadal climate oscillations over the North Pacific: Role in climatic regime shifts. *Geophys. Res. Lett.*, 26, 855-858.
- Minobe, S. and F.-F. Jin, 2004: Generation of interannual and interdecadal climate oscillations through nonlinear subharmonic resonance in delayed oscillators. *Geophys. Res. Lett.*, 31, L16206, doi:10.1029/2004GL019776.

- Nishikawa, H. and I. Yasuda, 2008: Japanese sardine (*Sardinops melanostictus*) mortality in relation to the winter mixed layer depth in the Kuroshio Extension region. *Fish. Oceanogr.* 17, 411–420.
- Nishikawa, H. and I. Yasuda, 2011: Long-term variability of winter mixed layer depth and temperature along the Kuroshio jet in a high-resolution ocean general circulation model. *J. Oceanogr.* 67, 503–518.
- Nishikawa, H., I. Yasuda, and S. Itoh, 2011: Impact of winter-to-spring environmental variability along the Kuroshio jet on the recruitment of Japanese sardine (*Sardinops melanostictus*). *Fish. Oceanogr.*, 20(6), 570–582.
- Nishikawa, H., I. Yasuda, S. Itoh, K. Komatsu, H. Sasaki, Y. Sasai and Y. Oozeki, 2013a: Transport and survival of Japanese sardine (*Sardinops melanostictus*) eggs and larvae via particle tracking experiments. *Fish. Oceanogr.*, 22(6), 509–522.
- Nishikawa, H., I. Yasuda, K. Komatsu, H. Sasaki, Y. Sasai, T. Setou and M. Shimizu, 2013b: Winter mixed layer depth and spring bloom along the Kuroshio front: implications for feeding environment and recruitment of Japanese sardine, *Mar. Ecol. Prog. Ser.*, 487, 217–229.
- Nishioka, J., T. Nakatsuka, Y.W. Watanabe, I. Yasuda, K. Kuma, H. Ogawa, N. Ebuchi, A. Scherbinin, Yu. N. Volkov, T. Shiraiwa, M. Wakatsuchi, 2013: Intensive mixing along an Island chain controls oceanic biogeochemical cycles. *Global Biogeochem. Cycles*, 27, 1–10, doi:10.1002/gbc.20088.
- Noto, M. and I. Yasuda, 1999: Population decline of the Japanese sardine, *Sardinops melanostictus*, in relation to sea surface temperature in the Kuroshio Extension. *Can. J. Fish. Aquat. Sci.* 56, 973–983.
- Noto, M. and I. Yasuda, 2003: Empirical biomass model for the Japanese sardine with sea surface temperature in the Kuroshio Extension. *Fish. Oceanogr.* 12, 1–9.
- Ono, K., K-I Ohshima, T. Kono, K. Katsumata, I. Yasuda, and M. Wakatsuchi, 2013: Distribution of vertical diffusivity in the Bussol' Strait: a mixing hot spot in the North Pacific. *Deep-Sea Res. I*, 79, 62–73.
- Osafune, S. and I. Yasuda, 2006: Bidecadal variability in the intermediate waters of the northwestern subarctic Pacific and the Okhotsk Sea in relation to 18.6-year period nodal tidal cycle. *J. Geophys. Res.*, 111, C05007, doi:10.1029/2005JC003277.
- Osafune, S. and I. Yasuda, 2010: Bidecadal variability in the Bering Sea and the relation with 18.6-year period nodal tidal cycle. *J. Geophys. Res.*, 115, DOI: 10.1029/2008JC005110.
- Osafune, S. and I. Yasuda, 2012: Numerical study on the impact of the 18.6-year period nodal tidal cycle on water-masses in the subarctic North Pacific. *J. Geophys. Res.-Oceans*, 117, C05009 DOI: 10.1029/2011JC007734.
- Osafune, S. and I. Yasuda, 2013: Remote impacts of the 18.6-year period modulation of localized tidal mixing in the North Pacific. *J. Geophys. Res. Oceans*. 118, 3128–3137.
- Tadokoro, K., T. Ono, I. Yasuda, S. Osafune, A. Shiimoto and H. Sugisaki, 2009: Possible mechanisms of decadal scale variations in PO₄ concentration in the Oyashio and Kuroshio-Oyashio Transition waters, western North Pacific. *Geophys. Res. Lett.* 36, L08606, doi:10.1029/2009GL037327.
- Takahashi, T., et al., 2002: Global sea–air CO₂ flux based on climatological surface ocean pCO₂ and seasonal biological and temperature effects. *Deep-Sea Research II*, 49, 1601–1622.
- Tanaka, T., I. Yasuda, K. Kuma and J. Nishioka, 2012: Turbulent iron flux sustains Green Belt along the shelf break in the southeastern Bering Sea. *Geophys. Res. Lett.*, 39, L08603 DOI: 10.1029/2012GL051164.
- Tanaka, T., I. Yasuda, Y. Tanaka, and G.S. Carter, 2013: Numerical study on tidal mixing along the shelf break in the Green Belt in the southeastern Bering Sea. *J. Geophys. Res. Ocean*, 118, 1–19, doi:10.1002/2013JC009113.
- Tanaka, T., I. Yasuda, H. Onishi, H. Ueno, and M. Masujima, 2015: Observations of current and mixing around the shelf break in Pribilof Canyon in the Bering Sea. *J. Oceanogr.*, 71, 1–17, DOI 10.1007/s10872-014-0256-2
- Tanaka, Y., I. Yasuda, H. Hasumi, H. Tatebe, S. Osafune, 2012: Effects of 18.6-year modulation of tidal mixing on bidecadal climate variability in the North Pacific. *J. Climate*, 25, 7625–7642.
- Tanaka, Y., I. Yasuda, S. Osafune, T. Tanaka, J. Nishioka and Y.N. Volkov, 2014: Internal tides and turbulent mixing observed in the Bussol Strait. *Progress in Oceanography*, 126, 98–108.
- Watanabe, Y., H. Zenitani, and R. Kimura, 1995: Population decline of the Japanese sardine *Sardinops melanostictus* owing to recruitment failures. *Can. J. Fish. Aquat. Sci.* 52, 1609–1616.
- Yagi M. and I. Yasuda, 2012: Deep intense vertical mixing in the Bussol' Strait. *Geophys. Res. Letters*, 39, L01602, doi:10.1029/2011GL050349.
- Yagi, M. and I. Yasuda, 2013: A method for estimating vertical profiles of turbulent dissipation rate using density inversions in the Kuril Straits. *J. Oceanogr.*, 69, 203–214, DOI 10.1007/s10872-012-0165-1
- Yagi, M., I. Yasuda, T. Tanaka, Y. Tanaka, K. Ono, K.I. Ohshima, K. Katsumata, 2014: Re-evaluation of vertical structure of turbulent mixing in the Bussol' Strait and its impact on water-masses in the Okhotsk Sea and the North Pacific. *Progress in Oceanography*, 126, 121–134.
- Yasuda, I., H. Sugisaki, Y. Watanabe, S. Minobe and Y. Oozeki, 1999: Interdecadal variations in Japanese sardine and ocean/climate. *Fish. Oceanogr.*, 8, 18–24.
- Yasuda, I., S. Osafune and H. Tatebe, 2006: Possible explanation linking 18.6-year period nodal tidal cycle with bi-decadal variations of ocean and climate in the North Pacific. *Geophys. Res. Letters*, 33, L08606, doi:10.1029/2005GL025237.
- Yasuda, I., 2009: The 18.6-year period moon-tidal cycle in Pacific Decadal Oscillation reconstructed from tree-rings in western North America. *Geophys. Res. Lett.*, 36, L05605, doi:10.1029/2008GL036880.

Observations of the Kuroshio Extension by an Autonomous Microstructure Float

Takeyoshi Nagai¹, Ryuichiro Inoue²,
Amit Tandon³, Hidekatsu Yamazaki¹

1. Department of Ocean Sciences, University of Marine Science and Technology, Tokyo, Japan
2. Ocean Circulation Research Group, Japan Agency for Marine-Earth Science and Technology, Yokosuka City, Japan
3. Department of Mechanical Engineering, University of Massachusetts Dartmouth, North Dartmouth, Massachusetts, USA

Introduction

The Kuroshio carries tremendous volume of water and transports large amount of heat, organic and inorganic constituents, impacting climate, storm tracks, and ocean ecosystems. The strong current of the Kuroshio is inherently associated with its frontal structures, with across frontal variations in temperature and salinity. Mixing of these water properties could lead to formations of new water masses, which could be subducted to ocean interior at fronts (Rudnick 1996; Nurser and Zhang 2000). Several studies have suggested that the Gulf Stream, a western boundary current in the North Atlantic, is a nutrient stream which transports nutrients from tropical ocean to subpolar regions in its subsurface layers (Pelegri and Csanady 1991; Pelegri et al. 1996). Recent studies have shown that the subsurface current of the Kuroshio is also a nutrient stream in the North Pacific (Guo et al. 2012 and 2013) similarly to the Gulf Stream. Stirring and mixing along the path of the Kuroshio, from the Kuroshio origin, its main stream off Japan coast, and the Kuroshio Extension, could, therefore, play important roles not only for physical oceanography and air-sea interactions but also for biogeochemistry.

Subinertial stirring due to mesoscale flows moves water parcels nearly along isopycnal, and, therefore, is not effective to stir density of the water across the front. However, when isopleths of temperature, salinity, and other tracers, for example nutrients, are not parallel to isopycnals, it is very efficient to stir these tracers resulting in numerous bands of streaks or filaments, with no density signatures, so called T-S compensated filaments (Rudnick and Ferrari 1999; Smith and Ferrari 2009). This is the case in the Kuroshio Extension Front, where the water parcels of same density consist of different temperature and salinity across the front. With strong baroclinicity and confluence in the Kuroshio, T-S compensated anomalous features can be subducted on the dense side and obducted on the light side of a front (Hoskins and Bretherton 1972). These T-S compensated filaments have been frequently observed as tongues across the Kuroshio Extension Front in

the high resolution surveys (Nagai et al. 2012). The subinertial stirring and associated filamentations increase tracer variance with reductions of filaments' spatial scales, cascading tracer variance to smaller scales until it dissipates at the molecular scale.

For the atmospheric fronts with the simultaneous deformation by horizontal confluence and vertical shear, Haynes and Anglade (1997) showed that the vertical diffusion process is the vital dissipater of the tracer variance, which, in turn, limits the horizontal scale of filaments. Using data obtained from the North Atlantic Tracer Release Experiment (NATRE; Ledwell et al. 1998), Ferrari and Polzin (2005) showed the average balance between thermal variance provided by mesoscale lateral stirring and average thermal dissipation below 800 m depth, where intermediate and Mediterranean waters convolve. Smith and Ferrari (2009) have also shown numerically that vertical mixing is important and sufficient to dissipate the tracer variance at these fine vertical scales, consistent with the atmospheric study of Haynes and Anglade (1997).

These previous atmospheric and oceanic studies suggest that the vertical diffusion of the vertical filaments plays a crucial role in determining the horizontal scale of the filaments. However, it has been unclear what vertical mixing mechanisms are responsible for dissipation of tracer variance.

Recent in situ observations in the thermocline under the main stream of the Kuroshio show large turbulent kinetic energy dissipation rates (Nagai et al. 2009), which are accompanied by near-inertial internal wave shear along isopycnals (Nagai et al. 2015a). Because near-inertial internal waves can be trapped and amplified by geostrophic shears (Kunze 1985; Mooers 1975; Whitt and Thomas 2013), enhanced turbulent dissipation with banded shear can be attributed to turbulence associated with these near-inertial waves under the Kuroshio. Even with no turbulence, tracers in the ocean can be mixed vertically by double-diffusive convection (Schmitt 1981; Schmitt and Georgi 1982; St. Laurent and Schmitt 1999; Merryfield 2005; Schmitt et al. 2005). Because T-S compensated filaments have no density signatures, it is very plausible that these filaments are in double-diffusive favourable conditions once they are formed vertically.

To observe these microscale mixing processes, tethered vertical microstructure profilers have been utilized. However, it is challenging to deploy such instruments within the strong baroclinic currents of the Kuroshio, because quasi freefall or free rising deployments, required for microstructure vertical profiling, are easily prevented by strong currents, their vertical shear, and varying wind conditions during the deployments. Untethered instruments, such as floats and gliders are more suitable to profile microstructure continuously under the Kuroshio main stream with their slow profiling speeds, $O(0.1 \text{ ms}^{-1})$.

In this study, a Navis-MicroRider microstructure float and an EM-APEX float were deployed along the Kuroshio Extension Front. The results of the observations indicate that vertical shear of near-inertial internal waves as well as subinertial flow can create interleaving thermohaline structures along the main stream of the Kuroshio Front, accompanied by very large microscale thermal dissipation rates with weak turbulence, suggesting that subinertial stirring and near-inertial shear promote double-diffusive convection and forward cascade of tracer variance.

Observations

In July 2013, an EM-APEX float (Teledyne Webb Research; Sanford et al. 2011) and a microstructure float were deployed at 37°N 20' 142°E 42', which were advected rapidly along the main stream of the Kuroshio Extension Front between 36°N and 37°N 30' (Figure 2g). A microstructure sensor package (MicroRider Rockland Scientific) and a battery pack were mounted externally on a Navis-Float (Sea-Bird Electronics) to integrate the microstructure float (Figure 1).



Figure 1: The microstructure float. A MicroRider (RSI Victoria Canada) is mounted on a Navis-Float (SBE).

The microstructure float carries two shear probes and two Fp07 thermistor sensors, to measure microscale vertical shear, and microscale temperature gradient at 512 Hz, respectively. The EM-APEX float measured absolute horizontal current velocity, temperature and salinity about every 2 hours for 500 m water column, and the microstructure float measured microstructures, temperature and salinity every 4 hours for 500 m water columns. Deployments of these two floats in the main stream of the Kuroshio Extension allowed us to obtain high-resolution velocity, microstructure, and hydrographic data along the Kuroshio Extension, while these floats traversed the meandering front rapidly to the downstream (Figure 2g). The microstructure float was recovered after about 3 days, while the EM-APEX float was kept profiling for over 10 days. Across the Kuroshio Extension Front, where two profiling floats were deployed, temperature, salinity, and current velocity were measured using a shipboard ADCP (38KHz Teledyne RDI) and a tow-yo CTD (Underway-CTD, Teledyne OceanScience).

Turbulent kinetic energy dissipation rates ϵ are computed by integrating the turbulent shear spectra where the spectra agree with the Nasmyth model spectrum (Nasmyth 1970). The shear spectra are converted to wave number spectra using the free-rising speed of the float, 0.11-0.26 ms^{-1} . Noises from the buoyancy pump of the float typically contaminate the turbulent shear signal for the bottom 100 m, and appear at frequencies higher than 30-40 Hz; moderate levels of turbulence, $O(>10^{-9} \text{ Wkg}^{-1})$, are not likely affected. The microscale thermal variance dissipation rate χ is obtained by integrating temperature gradient spectra for the range without electronic noise at higher frequency. With slow rising speeds of the float, the temperature gradient spectra show excellent agreement with Kraichnan spectrum (Kraichnan 1968).

Thermohaline structures and Microstructures

The measured along front flow of the Kuroshio Extension show a strong eastward current exceeding 1.5 ms^{-1} near the surface (Figure 2a). The across front flow is computed as the normal velocity component with respect to the Kuroshio axis, which is defined as the 500-m mean 30 hour lowpass filtered velocity obtained by the EM-APEX float. The computed across front velocity shows alternating positive and negative bands modulating with near-inertial frequencies (Figure 2b), indicating the strong influences from the near-inertial internal waves Thermohaline interleaving structures are observed in the across front Underway-CTD survey, with a characteristic cold low salinity tongue extending from north along isopycnal at $\sigma_\theta=26.25$ (Figure 2c). These interleaving structures are also found below 150 m depth, over 900 km along the Kuroshio Extension Front (Figure 2d and f). Spectral analyses show that along isopycnal rate of change in spiciness and vertical shear are correlated at subinertial and near-inertial frequencies, suggesting that the observed interleaving structures are modulated by subinertial and near-inertial shear (Nagai et al. 2015). Measured microscale thermal variance dissipation rates χ are very large $O(10^{-7}\text{-}10^{-6} \text{ K}^2\text{s}^{-1})$ between 150-400 m (Figure 2i) where the thermohaline interleaving structures are observed, while turbulent kinetic energy dissipation rates ϵ are relatively small $O(10^{-10}\text{-}10^{-9} \text{ W kg}^{-1})$ (Figure 2h). The trend that large χ and small ϵ is the indication of the possibility of the double-diffusive convection. Using Osborn model (Osborn 1980) and Osborn-Cox model (Osborn and Cox 1972), the turbulent eddy diffusivity for density and effective thermal diffusivity are computed by $K_\rho=\gamma\epsilon/N^2$, and $K_\theta=\chi/2(T_z)^2$, respectively, where γ is efficiency factor, 0.2, N buoyancy frequency, T_z background vertical temperature gradient.

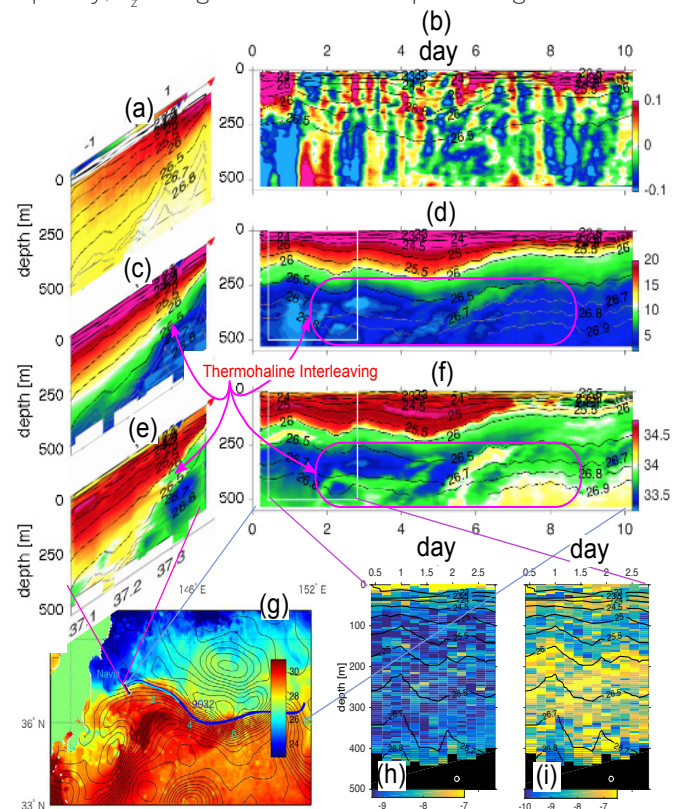


Figure 2: Across-frontal depth-latitude plots for (a) ADCP along-front flow (ms^{-1}), (c) potential temperature ($^{\circ}\text{C}$), and (e) salinity (PSU) measured by Underway-CTD along the observation line shown as solid black line in (g). Along-frontal depth-time plots of (b) across-front flow (ms^{-1}), (d) potential temperature ($^{\circ}\text{C}$), (f) salinity (PSU) measured by EM-APEX float along the Kuroshio Extension Front for 10 days. White boxes in (d and f) are time-depth ranges for (h) the turbulent kinetic energy dissipation rates ϵ and (i) microscale thermal variance dissipation rates χ measured by microstructure float.

Average effective thermal diffusivity K_θ between 150 and 400 m depth is $1.7 \times 10^{-3} \text{ m}^2\text{s}^{-1}$, which is 100 times larger than that for turbulent eddy diffusivity for density, K_ρ of $O(10^{-5} \text{ m}^2\text{s}^{-1})$. Computed Turner angles (Ruddick 1983) suggest that these large effective thermal diffusivity and χ with relatively small eddy diffusivity for density K_ρ and ϵ are found with double-diffusive favourable conditions (Nagai et al. 2015b). The derived effective thermal diffusivity is found to be consistent with the previous parameterizations for double-diffusive convection (Radko and Smith 2012; Fedorov 1988; Nagai et al. 2015b), suggesting further that the observed large thermal diffusivity is caused by double-diffusion.

In this study we observed thermohaline interleaving structures below 150 m depth along the Kuroshio Extension Front over 900 km with double-diffusive favourable conditions. Because the high correlations between vertical shear of subinertial and near-inertial frequencies and rate of change in spiciness are found, double-diffusive favourable thermohaline interleaving structures are likely to be formed both by subinertial and near-inertial shear. Within these thermohaline interleaving layers, larger microscale thermal variance dissipation rates $\chi \sim O(10^{-7}\text{-}10^{-6} \text{ K}^2\text{s}^{-1})$ and effective thermal diffusivity K_θ of $O(10^{-4}\text{-}10^{-3} \text{ m}^2\text{s}^{-1})$ are observed with small turbulent kinetic energy dissipation rates $\epsilon \sim O(10^{-10}\text{-}10^{-9} \text{ W kg}^{-1})$ and turbulent eddy diffusivity for density K_ρ of $O(10^{-5} \text{ m}^2\text{s}^{-1})$. The observed effective thermal diffusivity K_θ is found to be consistent with the previous double-diffusion parameterization, suggesting that the large microscale thermal variance dissipation rate χ is caused by double-diffusive convection. Accordingly, our results suggest that mesoscale subduction, obduction and near-inertial waves near oceanic fronts have catalytic effects to enhance subsurface double-diffusive convection. The enhanced thermal dissipation below the Kuroshio Extension with interleaving thermohaline structures suggests that double-diffusive convection is an important agent to dissipate tracer variance at microscales in subsurface layers of the Kuroshio Extension Front.

Acknowledgments

We thank Capt. Inoue, crews of R.V. Kaiyo (JAMSTEC), Mr. Okada at NME Ltd. for assists in field surveys, all those who participated in the cruise including Dr. Lueck at RSI, Dr. Li, Dr. Kokubu, Mr. Mabuchi at JFE-Advantech, Dr. Hasegawa at FRA, all the students and staff of the lab (Homma, Masunaga, Foloni-Neto, Yukawa, Nishi, Furuyama, Takeuchi, Nakamura, Sugata, Hohman, Allmon), Dr. Hosoda, Ms. Hirano and Mr. Nakajima at JAMSTEC, Mr. Dunlap at APL, and Dr. Mitchell and Mr. Quittman at SBE for the float configuration and operations, Dr. Wolk and Mr. Stern at RSI, and Mr. Yazu at JFE-Advantech for the MicroRider integrations, Ms. Lynn Allmon for editorial assistance, and Prof. Ruddick and Dr. Schmitt for their insights. TN thanks JSPS (KAKENHI 24684036), "The Study of Kuroshio Ecosystem Dynamics for Sustainable Fisheries (SKED)" funded by MEXT, MIT-Hayashi Seed Fund. AT thanks NSF-1434512 and ONR-N000141310456 for support."

References

Fedorov, K. N., 1988: Layer tickles and effective diffusivities in diffusive thermohaline convection in the ocean, In: Small-scale turbulence and mixing in the ocean, J. Nihoul and B. Jamart (Eds.), 247 pp., Elsevier.

Ferrari, R., and K. L. Polzin, 2005: Finescale structure of the T-S relation in the Eastern North Atlantic, *J. Phys. Oceanogr.*, 35, 1437–1454.

Guo, X., X.-H. Zhu, Q.-S. Wu, and D. Huang, 2012: The Kuroshio nutrient stream and its temporal variation in the East China

Sea, *J. Geophys. Res.*, 117, C01026, doi:10.1029/2011JC007292.

Guo, X., X.-H. Zhu, Y. Long, and D. J. Huang, 2013: Spatial variations in the Kuroshio nutrient transport from the East China Sea to south of Japan, *Biogeosciences*, 10, 6403–6417.

Hoskins, B. J., and F. P. Bretherton, 1972: Atmospheric frontogenesis models: Mathematical formulation and solution, *J. Atmos. Sci.*, 29, 11–37.

Haynes, P., and J. Anglade, 1997: The vertical-scale cascade in atmospheric tracers due to large-scale differential advection, *J. Atmos. Sci.*, 54, 1121–1136.

Kraichnan, R., 1968: Small-scale structure of a scalar field convected by turbulence, *Phys. Fluids*, 11, 945–953.

Kunze, E., 1985: Near-inertial wave propagation in geostrophic shear, *J. Phys. Oceanogr.*, 15, 544–565.

Ledwell, J. R., A. J. Watson, and C. S. Law, 1998: Mixing of a tracer in the pycnocline, *J. of Geophys. Res.*, 103 (C10), 21,499–21,529, doi:10.1029/98JC01738.

Merryfield, B., 2005: Ocean mixing in 10 steps, *Science*, 308, 641–642.

Mooers, C. N., 1975: Several effects of baroclinic current on the cross-stream propagation of inertial-internal waves, *Geophys. Fluid Dyn.*, 6, 245–275.

Nagai, T., A. Tandon, H. Yamazaki, and M. J. Doubell, 2009: Evidence of enhanced turbulent dissipation in the frontogenetic Kuroshio Front thermocline, *Geophys. Res. Lett.*, 36, L12,609, doi:10.1029/2009GL038832.

Nagai, T., A. Tandon, H. Yamazaki, M. J. Doubell, and S. Gallager, 2012: Direct observations of microscale turbulence and thermohaline structure in the Kuroshio Front, *J. Geophys. Res.*, 117, C08,013, doi:10.1029/2011JC00722.

Nagai, T., A. Tandon, E. Kunze, and A. Mahadevan, 2015a: Spontaneous generation of near-inertial waves by the Kuroshio Front, *J. Phys. Oceanogr.* 45, 2381–2406.

Nagai, T., R. Inoue, A. Tandon, and H. Yamazaki, 2015b: Evidence of enhanced double-diffusive convection below the main stream of the Kuroshio Extension, *J. Geophys. Res. Oceans*, 120, 8402–8421, doi:10.1002/2015JC011288.

Nasmyth, P. W., 1970: Oceanic turbulence, Ph.D. thesis, University of British Columbia.

Nurser, A. J. G., and J. W. Zhang, 2000: Eddy-induced mixed layer shallowing and mixed layer/thermocline exchange, *J. Geophys. Res.*, 105, 21,851–21,868.

Osborn, T., 1980: Estimates of the local rate of vertical diffusion from dissipation measurements, *J. Phys. Oceanogr.*, 10, 83–89.

Osborn, T. R., and C. S. Cox, 1972: Oceanic fine structure, *Geophys. Fluid Dyn.*, 3, 321–345.

Pelegri, J. L., and Csanady, G. T., 1991: Nutrient transport and mixing in the Gulf stream. *J. Geophys. Res.* 96(C2), 2577–2583.

Pelegri, J. L., Csanady, G. T., and Martins, A., 1996: The north Atlantic nutrient stream. *J. Oceanogr.* 52, 275–299.

Radko, T., and D. P. Smith, 2012: Equilibrium transport in double-diffusive convection, *J. Fluid Mech.*, 692, 5–27.

Ruddick, B. R., 1983: A practical indicator of the stability of the water column to double-diffusive activity, *Deep Sea Res.*, 30, 1105–1107.

Rudnick, D. L., 1996: Intensive surveys of the Azores front. Part II: Inferring the geostrophic and vertical velocity fields, *J. Geophys. Res.*, 101, 16,291–16,303.

Rudnick, D. L., and R. Ferrari, 1999: Compensation of horizontal temperature and salinity gradients in the ocean mixed layer, *Science*, 283(5401), 526–529, doi: 10.1126/science.283.5401.526.

Sanford, T. B., J. F. Price, and J. B. Girton, 2011: Upper-ocean response to hurricane Frances (2004) observed by profiling EM-APEX floats, *J. Phys. Oceanogr.*, 41, 1041–1056.

Schmitt, R. W., 1999: Spice and the demon, *Science*, 283, 498–499.

Schmitt, R. W., and D. Georgi, 1982: Finestructure and microstructure in the North Atlantic Current., *J. Mar. Res. (Suppl.)*, 40, 659–705.

Schmitt, R. W., J. R. Ledwell, E. T. Montgomery, K. L. Polzin, and J. M. Toole, 2005: Enhanced diapycnal mixing by salt fingers in the thermocline of the tropical Atlantic, *Science*, 308(5722), 685–688, doi:10.1126/science.1108678.

Smith, K. S., and R. Ferrari, 2009: The production and dissipation of compensated thermohaline variance by mesoscale stirring, *J. Phys. Oceanogr.*, 39, 2477–2501.

St. Laurent, L. C., and R. W. Schmitt, 1999: The contribution of salt fingers to vertical mixing in the North Atlantic Tracer Release Experiment, *J. Phys. Oceanogr.*, 29, 1404–1424.

Whitt, D., and L. Thomas, 2013: Near-inertial waves in strongly baroclinic currents, *J. Phys. Oceanogr.*, 43, 706–725.

Observational and Numerical Study of the Frontal- and Mesoscale Air-Sea Interaction in the Kuroshio Extension Region in the North Pacific

Xiaopei Lin¹, Xiaohui Ma^{2,1}, Zhaohui Chen¹, Lixiao Xu¹, Xue Liu^{2,1}, Zhao Jing^{2,1}, Lixin Wu¹, Dexing Wu¹, Ping Chang^{2,1}

1. Physical Oceanography Laboratory/CIMSST, Ocean University of China and Qingdao National Laboratory for Marine Science and Technology, Qingdao, China
2. Department of Oceanography, Texas A&M University

Introduction

The Kuroshio extension region has been identified as a key location in the extratropics in the North Pacific where sharp oceanic fronts and energetic mesoscale oceanic eddies induce considerable sea surface temperature (SST) variability, leading to intensive air-sea interaction. Understanding these frontal- and mesoscale air-sea interaction has important implications to improve future climate modelling, prediction and application at the midlatitude. However, quantifying and understanding this air-sea coupling have proven to be formidable challenges for a number of reasons. First, as one of the strongest western boundary currents, the Kuroshio extension is the region where both atmosphere and ocean are dynamically unstable, producing energetic eddies that tend to mask the ocean-atmosphere feedback signals. Second, unlike the tropics where ocean-atmosphere interaction occurs in basin-to-global scale, the interaction in the Kuroshio extension region takes place along narrow frontal zones where the SST gradient is strong. There is generally a lack of understanding of small-scale processes in the ocean and atmosphere. Third, until very recently, available observations and numerical modelling tools were inadequate to resolve such small-scale dynamical processes in western boundary current regimes, making it difficult to further investigate the frontal- and mesoscale air-sea interaction. As a contribution to the ongoing effort, we aim to develop a sustainable observational network

through an international cooperation, establish a theoretical framework of the multi-scale ocean-atmosphere interactions in the Kuroshio extension region using eddy-resolving high-resolution coupled regional climate model, reveal key physical processes in determining climate changes, and improve the ocean and climate predictability in the North Pacific.

Observational Network

Until recently, there have been quite limited high-resolution observations in the Kuroshio extension region. One project providing systematic observational data is the Kuroshio Extension System Study (KESS), launched from 2004 to 2006 and funded by US National Science Foundation (NSF), which deployed an observing array consisting of Argo profiling floats, moored-profiler, moorings, Current-Pressure equipped Inverted Echo Sounder (CPIES) as well as a surface buoy (KEO) located south of the Kuroshio (Figure 1). North of the Kuroshio, another buoy (JKEO) was deployed by the Japan Agency for Marine-Earth Science and Technology (JAMSTEC)'s Institute in 2007. However, JKEO has been discontinued after the end of the Japanese HOTSPOT project in 2015. Following KESS and Japanese HOTSPOT projects, a new observational plan in the Kuroshio extension region under Intergovernmental Oceanographic Commission (IOC) Sub-Commission for the Western Pacific (WESTPAC), Air-Sea Interaction in the Kuroshio Extension and its Climate Impact (AIKEC) led by the Ocean University of China (OUC) and the Texas A&M University (TAMU), was setup to maintain continuous and sustainable observations in this region. Supported by the Ministry of Science and Technology of China, the Natural Science Foundation of China and the Qingdao National Laboratory for Marine Science and Technology, systematic observations in the Northwestern Pacific Ocean are being carried out during four cruises from 2014 to 2016 conducted by OUC. A summary of these cruises is shown in Figure 1. Two moorings have been deployed during the past two years: south of the Kuroshio extension where most of cold oceanic eddies occur, the M1 mooring has been placed near NOAA KEO buoy, so that the flux measurement can be combined with oceanic measurements to quantify the importance of interaction between oceanic eddy and atmosphere in this region; north of the Kuroshio extension where most of warm oceanic eddies and the most intensive mesoscale air-sea couplings occur, the M2 mooring has been deployed in the 2016 cruise, where a new surface flux buoy, named CKEO, will be placed in the following year so that mesoscale air-sea interaction dynamics in the region are regarded as a contrast with those in the south of the Kuroshio extension. In our future plan, CPIES will be deployed near M1 and M2 moorings to measure the high-resolution current, which assist to study the energy cascading of the small scale oceanic eddies. In addition, gliders will be flown repeatedly between M1 and M2 moorings in the future cruises.

With respect to the completed cruises, we have done a lot of work in the Kuroshio extension region. The 2014 research cruise took place from 17 March to 23 April 2014, and it was carried out by the research vessel "Dong Fang Hong 2". In the 38-day voyage, researchers deployed 25 sets of Argo floats and, for the first time in China, a deep-sea (6000m) mooring system (M0) in the Kuroshio extension region (Figure 1). In November 2015, another deep-sea mooring (M1) with McLane Moored Profiler (MMP) mounted was deployed and successfully recovered in the 2016. The 2016 cruise also deployed another subsurface mooring at the same location (M1) and a new subsurface mooring in the north of the Kuroshio Extension in the east of JKEO (M2). In addition to subsurface moorings, hundreds of radiosondes and Conductivity-Temperature-Depth (CTD) casts have been conducted during the previous cruises to profile the atmospheric

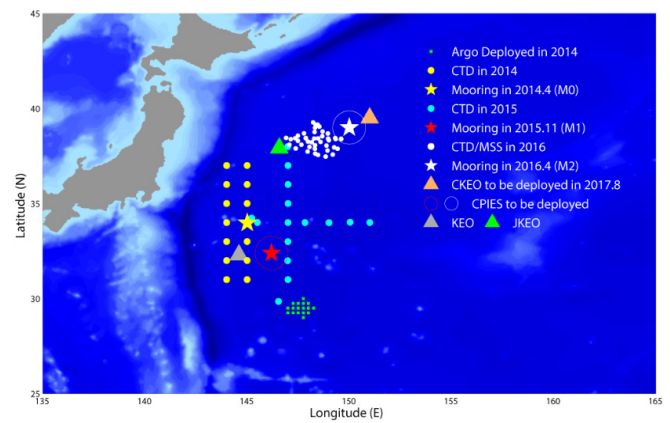


Figure 1: Moorings, Buoys and CTD/Argo/MSS positions in the new observation plan.

boundary layer, lower troposphere and the upper-layer ocean.

Numerical Models

A Coupled Regional Climate Model (CRCM) (Ma et al. 2016) has been developed by TAMU and OUC over the past several years, leveraging existing community model development activities, particularly the climate version of the Weather Research Forecast (WRF) Model developed at the US National Center for Atmospheric Research (NCAR), and the Regional Ocean Modeling System (ROMS) developed at Rutgers University and University of California - Los Angeles (UCLA). The use of these models offers a standardized means for coding and reporting and will greatly facilitate sharing results with the broader climate modelling community. Within the coupler, the atmosphere and ocean exchange surface fluxes at each coupling step. In current model configuration in the North Pacific, the surface fluxes are computed by WRF using modified bulk drag and enthalpy coefficients to improve accuracy in high-wind regimes. Surface stress formula is also modified to account for ocean surface velocity. Air-sea coupling frequency is typically set at one hour in the standard configuration to resolve diurnal cycle, but higher or lower frequencies may be used. The model includes a novel feature of spatially filtering SST at each coupling step that allows suppressing frontal- and mesoscale air-sea coupling. CRCM and its component models can be forced with observed data sets or global model simulation outputs at the lateral boundaries to produce an estimate of the climate state at high spatial resolution. The model has been widely tested in our study and applied in western boundary current regions including the Kuroshio extension in the North Pacific and the Gulf Stream in the North Atlantic. Results of the simulations are very encouraging and produce realistic Kuroshio (Gulf Stream) path, oceanic eddies and storm track variability in the North Pacific (Atlantic). In addition, the CRCM model shows great ability in forecasting the path of Hurricane Isaac in 2012.

Research Activities

Three research projects related to the study of the Kuroshio extension were funded in China, focusing on the response to global warming and regulation of climate change by the Pacific and Indian Oceans, multiscale variations, mechanisms and predictability of the Northwest Pacific Ocean, and climatic impacts of ocean-atmosphere interaction in the Kuroshio and its extension region.

During the Pacific Mode-Water Ventilation Experiment (P-MoVE; Xie 2013), 17 Argo profiling floats with enhanced daily sampling were deployed in an anticyclonic eddy region south of the Kuroshio extension in late March 2014.

More than 3,000 hydrographic Argo profiles following the anticyclonic eddy were obtained, offering an unprecedented detailed observational view of eddy subduction process in the region for the first time (Xu et al. 2016).

To understand the role of extreme heat flux events associated with atmospheric synoptic storms in frontal-scale air-sea interactions in the western boundary current regions, and its relationship with large-scale atmospheric variability, we have completed a comprehensive analysis of boreal winter extreme flux events in the Kuroshio Extension Region (KER) of the Northwestern Pacific and the Gulf Stream Region (GSR) of the Northwestern Atlantic, based on reanalysis and observationally data sets (Ma et al. 2015a). The results show that there is a close relationship between the extreme flux events over KER/GSR and the East Atlantic Pattern (EAP)/Pacific Decadal Oscillation (PDO), with more/less frequent occurrence of the extreme flux events during a positive/negative EAP/PDO phase. Moreover, ALP/EAP can be explained as accumulated effects of the synoptic winter storms accompanied with the extreme flux events.

To investigate the extent that frontal- and mesoscale SST associated with ocean mesoscale eddies can impact the atmosphere locally and remotely (Figure 2.), we have completed a suite of high-resolution regional climate model WRF simulations in North Pacific domain at various spatial resolutions ranging from 9 km, 27 km and to 162 km. Mesoscale SST variability associated with oceanic eddies not only can have a major impact within and above the atmosphere boundary layer locally (Figure 2.), but more importantly can exert remote influence on basin-scale atmosphere circulation. Mesoscale SST variability, though largely confined in the Kuroshio extension region, can affect local cyclogenesis and downstream storm development, which further exert a significant distant influence on winter rainfall variability along the U. S. Northern Pacific coast, as well as a remote barotropic mean flow response in the eastern North Pacific. A new theory on midlatitude SST influence on the atmosphere has been formulated based on the concept of moist baroclinic instability: the presence of mesoscale SST anomalies enhances the diabatic conversion of latent heat energy to transient eddy energy, intensifying winter cyclogenesis via moist baroclinic instability, which in turn affects downstream stormtrack and precipitation (Ma et al. 2015b). This finding points to the potential of improving forecasts of extratropical winter cyclones and storm systems and projections of their response to future climate change, which are known to have major social and economic impacts, by improving the representation of ocean eddy-atmosphere interaction in forecast and climate models.

Summary and Work Underway

Major progress has been made during the last three years (2012-2015), including three Chinese national research projects focusing on the air-sea interaction study in the Kuroshio extension region and two research cruises in the Northwestern Pacific Ocean. The accomplishment of these activities not only improves our understanding of frontal- and mesoscale air-sea interaction at midlatitude and provides scientific support for the enhancement of prediction capability of climate models, but also promotes interdisciplinary integration as well as international communication and cooperation in observation and research in the western boundary current regions.

The 2016 research cruise has taken place from March 22 to May 3 to deploy another deep-sea mooring, while a newly-developed buoy CKEO north of the Kuroshio will be deployed in the following year. However, international collaborations are highly desired to perform long-term mooring maintenance. The CKEO flux buoy will be built as a joint venture between China and NOAA/PMEL's or GERG/TAMU. Data collection during these regular cruises and the mooring data will contribute to build a systematic observation network in the Kuroshio extension region in the future.

There are also several important scientific questions related to frontal- and mesoscale air-sea interaction in the Kuroshio extension region and will be addressed in a future study. First, we intend to investigate the feedback mechanism governing ocean mesoscale eddy-atmosphere interaction and its role in affecting large-scale atmosphere and ocean circulation. This has been done by conducting an ensemble of high-resolution eddy-resolving CRCM simulations for both the atmosphere and ocean, with and without mesoscale SST signatures in the North Pacific. Second, we will carry out Lagrangian analyses of ocean mesoscale eddies in the Kuroshio extension regions using an objective eddy-recognition algorithm. These analyses will examine atmospheric responses following the identified ocean eddies and its feedback on oceanic eddies, and compare the responses between warm and cold ocean eddies. These analyses can also help address whether the atmospheric responses to warm and cold eddies are asymmetric, leading to a rectified effect of eddies on the atmosphere. Finally, we will attempt to construct simple empirical models of the mesoscale ocean-atmosphere feedback based on high-resolution coupled simulations, and parameterize its effect in coarse-resolution climate models used for long-term integrations, in order to reduce the climate model bias by correctly representing the mesoscale air-sea coupling.

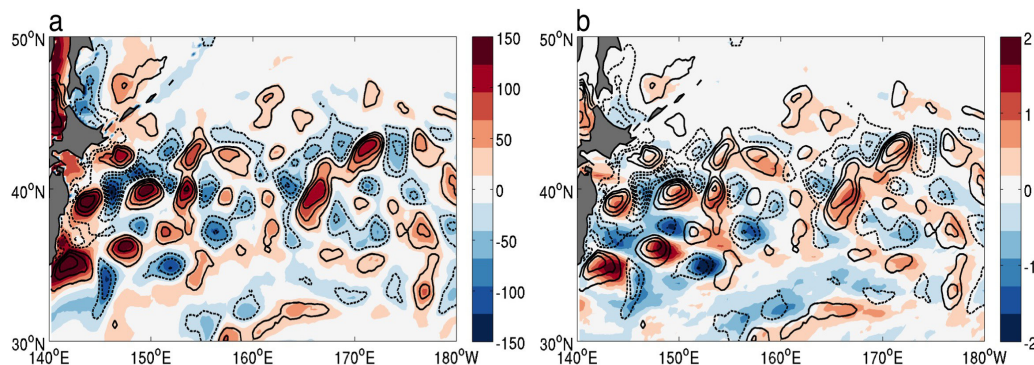


Figure 2: Winter season mean (NDJFM) (a) spatially high-pass filtered SST (contour, °C) and turbulent heat flux (color shaded, w^2/m) (b) spatially high-pass filtered SST (contour, °C) and convective rainfall (color shaded, mm/day) derived from 10 members ensemble mean of 27km WRF simulations.

References

Ma, X., Z. Jing, P. Chang, X. Liu, R. Montuoro, R. J. Small, F. O. Bryan, R. J. Greatbatch, P. Brandt, D. Wu, X. Lin and L. Wu, 2016: Western Boundary Currents regulated by interaction between ocean eddies and the atmosphere. *Nature*, Accepted.

Ma, X., P. Chang R. Saravanan, D. Wu, X. Lin, L. Wu, 2015a: Winter Extreme Flux Events in the Kuroshio and Gulf Stream Extension Regions and Relationship with Modes of North Pacific and Atlantic Variability, *J. Clim.*, 28, 4950-4970. doi: <http://dx.doi.org/10.1175/JCLI-D-14-00642.1>

Ma, X. H., P. chang, R. Saravanan, M. Raffaele, J. S. Hsieh, D. Wu, X. Lin, L. Wu and Z. Jing, 2015b: Distant Influence of Kuroshio Eddies on North Pacific Weather Patterns? *Scientific Reports*, 5, 17785 ,doi:10.1038/srep17785.

Xie, S.-P., 2013: Advancing climate dynamics toward reliable regional climate projections. *Journal of Ocean University of China*, 12, 191-200.

Xu, L., P. Li, S.-P. Xie, Q. Liu, C. Liu, and W. Gao, 2016: Observing mesoscale eddy effects on mode-water subduction and transport in the North Pacific. *Nature communications*, 7.

Effects of Deep Bottom Topography on the Kuroshio Extension Studied by a Nested-grid OGCM

Masao Kurogi¹, Yukio Tanaka, and Hiroyasu Hasumi²

1. Japan Agency for Marine-Earth Science and Technology, Yokohama, Japan
2. Atmosphere and Ocean Research Institute, The University of Tokyo, Kashiwa, Japan

Introduction

The Kuroshio is the western boundary current of the North Pacific subtropical gyre. After separating from the coast of Japan, its extension is called the Kuroshio Extension (KE). There are two quasi-stationary meanders in the KE path that can be seen in Figure 1a. Eddy activity in the KE region is high (Figure 1b) and the KE system is known to oscillate between stable states with low eddy activity and unstable states with high eddy activity on the decadal scale (Qiu and Chen, 2005).

Previous studies pointed out the effects of bottom topography on the KE path states. In the upstream region, the Kuroshio and KE flow on the Izu-Ogasawara Ridge and deep trench just east of it (see Figure 2a). Qiu and Chen (2005) pointed out that the KE path becomes unstable when the KE migrates southward and the KE inflow rides over shallow region of the Izu-Ogasawara Ridge. East of the trench, there is a vast abyssal plain with gradual undulation and seamounts. According to Hurlburt et al. (1996), such abyssal plain and seamounts are important for formation of the KE quasi-stationary meanders. Downstream of this region, the KE encounters the Shatsky Rise. Qiu and Chen (2010) suggested the influence of the Shatsky Rise on the KE path. That is, when the KE migrates southward and rides over shallow portion of it, disturbance is generated and the upstream KE is destabilized.

The maximum depth widely used in eddy-resolving simulations of (quasi) global Ocean General Circulation Models (OGCMs) lies mostly between 5500 m and 6000 m (e.g., Maltrud and McClean, 2005; Sasaki et al., 2008; Maltrud et al., 2010). Setting the maximum depth in models at 5500 m is enough to represent characteristic topography such as the Izu-Ogasawara Ridge, Shatsky Rise, and seamounts in the KE region. However, the undulation of vast abyssal plain mentioned above cannot be represented. The characteristic wavelength of large-scale abyssal undulation in this region is roughly 500-1000 km. As pointed out by Treguier and McWilliams (1990), it is expected that the effect of bottom topography decreases with the e-folding scale of f/NK , where f is the Coriolis parameter, N is the Brunt-Väisälä frequency, and K is the horizontal wavenumber. A rough estimate of this scale implies that the effects of such

large-scale topography penetrate to the upper ocean. In this study, the effects of such deep bottom topography on the KE are investigated by using a nested-grid eddy-resolving OGCM.

Description of Model and Experiments

The model used in this study is a two-way nested-grid OGCM based on an ice-ocean coupled model, named COCO (Hasumi, 2006). An inner model of the western North Pacific region (116°E-172°W, 14.3°N-52.9°N) is nested into the outer model covering the whole North Pacific (105°E-75°W, 14.8°S-67.7°N). The horizontal resolution of inner and outer models is $0.1^\circ \times 0.1^\circ \cos\theta$ and $0.5^\circ \times 0.5^\circ \cos\theta$, respectively, where θ is the latitude. There are 74 vertical levels with thickness increasing from 5 m at the surface to 200 m at the maximum depth of 9200 m.

The two-way nesting method adopted here is basically the same as that of Kurogi et al. (2013) with exception of the following two improvements. Firstly, a two-way coupling between the models is realized for all processes including calculations of sea ice. This enables smooth connection of sea ice variables across the interfaces between the models and stable calculation of sea ice. The second improvement is the implementation of conservative method similar to Debreu et al. (2012). At the grid interface, flux of an outer model grid is fitted to the value obtained by summing fluxes of inner model grids facing the same range of the interface. By applying such technique in realistic settings, Debreu et al. (2012) could not stably integrate the model with a terrain-following vertical coordinate. Our model with (basically) the geopotential height vertical coordinate was successful in performing a stable integration with realistic setting as described above.

Two experiments are executed by changing bottom topography. For the first case, deep bottom topography to the depth of 9200 m is represented (Figure 2a, hereafter called as EX9200). In the second case, bottom topography only to the depth of 5450 m is represented (hereafter called as EX5450). In this case, most part of the KE region upstream of the Shatsky Rise is flat (Figure 2b). For both experimental cases, the model is integrated from 1950 to 2009 with CORE Ver. 2 Interannual forcing (Large and Yeager, 2009). Relative wind is used to calculate wind stress for realistic representation of eddy activities in the Kuroshio and KE region (Tsuji et al., 2013). Results of the last 16 years (1993-2008) are compared.

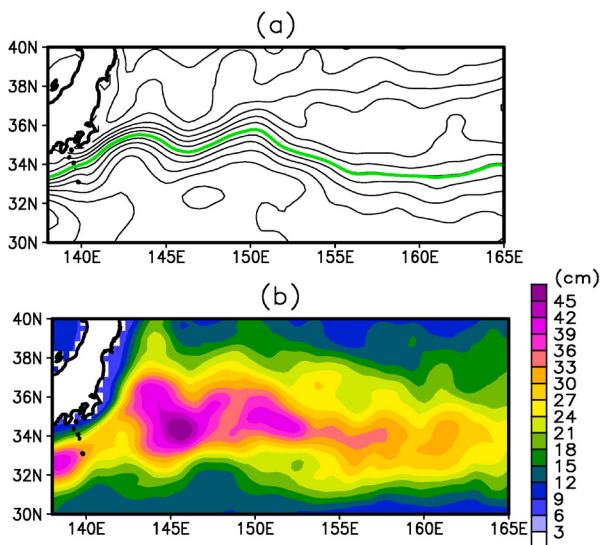


Figure 1: (a) Time-averaged SSH and (b) RMS of SSHA during 1993-2008 for observations with altimeter data. Contour interval in (a) is 10 cm. Green line in (a) indicates the KE axis defined by contour line of SSH with value of its regional average (141°E-153°E, 30°N-40°N).

Effects of deep bottom topography on the KE

Deep bottom topography in the KE region has a great impact on the time-averaged sea surface height (SSH) field. In EX9200 with deep topography (Figure 2c), the zonal location of crests of the KE meanders (around 144°E, 150°E) and the meander amplitude (about 130 km, defined here by amplitude in latitudinal direction of the quasi-stationary meanders) are close to observations (Figure 1a), though the simulated KE flows about $0.5\text{--}1^\circ$ northward compared to observations. The zonal location of crests of the KE meanders is almost the same in EX5450 without deep topography (Figure 2d). However, the amplitude of the KE meanders in this case is decreased by half.

Deep bottom topography also affects the strength and horizontal distribution of the eddy activity. The regional average (141°E-165°E, 30°N-40°N) of root-mean-square (RMS) of sea surface height anomaly (SSHA) (bottom panels of Figure 2) is 13 % larger in EX9200 (21.4 cm) compared to EX5450 (18.9 cm), and the former is closer to observations (22.4 cm). RMS of SSHA reaches maximum around 146° E and decreases gradually to the east in observations (Figure 1b). The regional average of RMS of SSHA in downstream region (153°E-165°E, 30°N-40°N) is 13 % smaller than that in the upstream region (141°E-153°E, 30°N-40°N) for observations. For the simulated KE, the regional average in the downstream region tends to be larger compared to that in the upstream region especially for EX5450 (13% larger) than for EX9200 (4% larger). Further, the region with high RMS of SSHA in EX5450 (Figure 2f) is much narrower than in observations (Figure 1b) and EX9200 (Figure 2e). As a whole, simulated distribution of RMS of SSHA is closer to the observations in the case with deep bottom topography.

The upper panels of Figure 3 show the upstream KE path length between 141°E and 153°E. This length is introduced by Qiu and Chen (2005) as an index of stability of the KE and shorter (longer) path length indicates stable (unstable) KE states. The upstream KE path length is shorter in EX5450 (1352 ± 219 km) than in EX9200 (1593 ± 319 km) and observations (1743 ± 465 km), reflecting the difference of eddy activity that RMS of SSH of the upstream region is higher in observations (23.9 cm) and EX9200 (21.0 cm) than in EX5450 (17.8 cm). Shorter path length in EX5450 is also due to the reduced amplitude of the quasi-stationary meanders because the upstream KE path length for time-averaged SSH (green line in Figure 1a, 2c and 2d) is 2-7% smaller in EX5450 (1187 km) than in EX9200 (1276 km) and observations (1214 km).

Time variation of the upstream KE path length is different between experimental cases. There is interannual variability in the upstream KE path length in EX9200 (Figure 3b) though the phase does not agree well with observations (Figure 3a). The upstream KE path length in EX5450 is almost shorter than observational time-averaged value and variation is much smaller than observations and EX9200 except around 2007 (Figure 3c). In this case, stable states are dominant. The middle panels of Figure 3 show the spaghetti diagram of the KE path for the year in stable states. The upstream KE path in stable states is similar to observations though the amplitude of the KE meander in EX5450 (Figure 3f) is smaller compared to observations (Figure 3d) and EX9200 (Figure 3e). For unstable states of the KE, the simulated KE path (Figure 3h and 3i) in the upstream region is convoluted compared to stable state (Figure 3e and 3f) but less convoluted to observations (Figure 3g).

Summary and discussion

It is found that deep bottom topography has a profound effect on the KE. By representing bottom topography deeper than

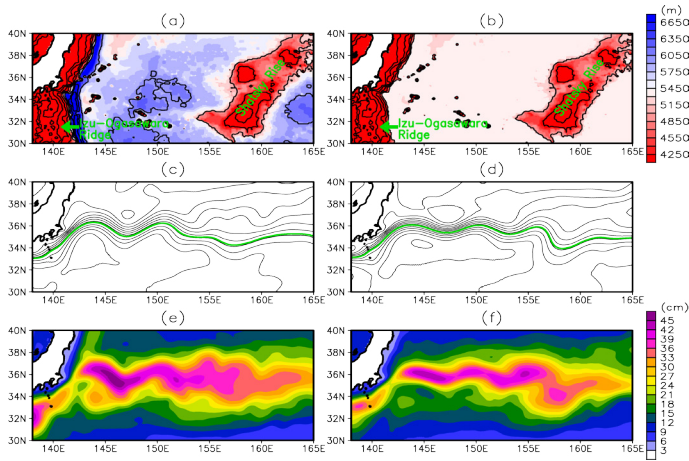


Figure 2: Bottom topography (top panels), time-averaged SSH (middle panels), and RMS of SSHA (bottom panels) for experimental cases. Left and right panels are for EX9200 and EX5450, respectively. Contour interval in (a-b), (c-d) are 1000 m, 10 cm, respectively. Green line in (c-d) indicates the KE axis.

5450 m, the amplitude of the KE quasi-stationary meanders and RMS of SSHA are enhanced. The upstream KE path length also becomes longer with its variability enhanced in the case with deep bottom topography. The detailed mechanism how deep bottom topography affects the KE is under investigation.

To better represent and understand the KE, there are remaining issues. For example, the simulated KE in unstable states is less convoluted compared to observations. This may be related to northward positioned path of the simulated KE. The KE tend to flow north of shallow portion of the Shatsky Rise which is pointed

out to destabilize the KE (Qiu and Chen, 2010). Effects of shallow portion of the Shatsky Rise will be clear in an experiment with this shallow region is extended northward to interact the KE jet. We are planning to execute such additional experiments to better understand the effects of bottom topography on the KE.

Acknowledgements

Figure 1 and left panels of Figure 3 are drawn using the altimeter products produced by Ssalto/Duacs and distributed by Aviso, with support from Cnes. This work is supported by Strategic Programs for Innovative Research (SPIRE) Field 3 of the Ministry of Education, Culture, Sports, Science, and Technology (MEXT), Japan. This work is also supported by the FLAGSHIP2020, MEXT within the priority study4 (Advancement of meteorological and global environmental predictions utilizing observational "Big Data"). Numerical simulations were conducted by using computational resources of the K computer provided by the RIKEN Advanced Institute for Computational Science through the HPCI System Research project (Project ID: hp120279, hp130010, hp140219, hp150213, hp150287, and hp160230).

References

Debreu, L., P. Marchesiello, P. Penven, and G. Cambon, 2012: Two-way nesting in split-explicit ocean models: Algorithms, implementation and validation. *Ocean Modell.*, 49–50, 1–21.

Hasumi, H., 2006: CCSR Ocean Component Model (COCO) version 4.0. CCSR Rep. 25, Center for Climate System Research, University of Tokyo, 103 pp.

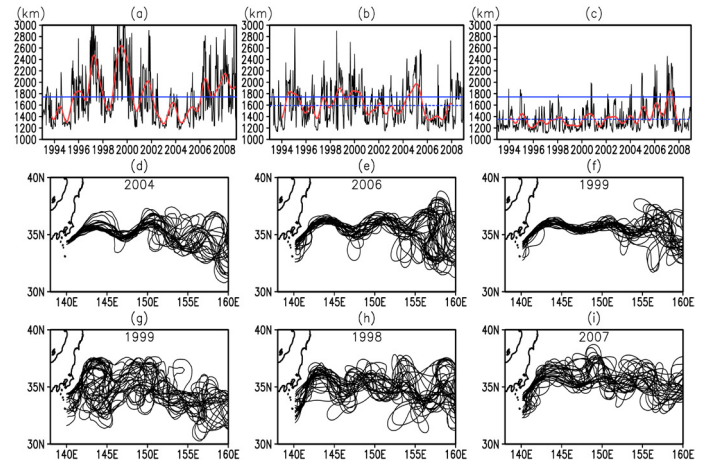


Figure 3: The length of KE path (axis) between 141°E and 153°E (top panels). The KE path (axis) for every 14 days in the year with the shortest KE path length (middle panels) and the longest KE path length (bottom panels). Corresponding year is indicated in the each panel. Left, middle and right panels are for observations with altimeter data, EX9200 and EX5450, respectively. Red and blue (dotted) lines in the top panels indicate low-pass filtered path length with time scale longer than 356 days and time-averaged path length for observations (each experimental case), respectively.

Kurogi, M., H. Hasumi, and Y. Tanaka, 2013: Effects of stretching on maintaining the Kuroshio meander. *J. Geophys. Res.*, 118, 1182–1194.

Large, W. G., and S. G. Yeager, 2009: The global climatology of an interannually varying air-sea flux data set, *Clim. Dyn.*, 33, 341–364.

Maltrud, M. E. and J. L., McClean, 2005: An eddy-resolving global 1/10° ocean simulation. *Ocean Modell.*, 8, 31–54.

Maltrud, M. and F. Bryan, S. Peacock, 2010: Boundary impulse response functions in a century-long eddying global ocean simulation. *Environ. Fluid Mech.*, 10, 275–295.

Qiu, B., and S. Chen, 2005: Variability of the Kuroshio extension jet, recirculation gyre, and mesoscale eddies on decadal time scales, *J. Phys. Oceanogr.*, 35, 2090–2103.

Qiu, B., and S. Chen, 2010: Eddy-mean flow interaction in the decadal modulating Kuroshio Extension system. *Deep-Sea Res. II*, 57, 1098–1110.

Sasaki, H., M. Nonaka, Y. Masumoto, Y. Sasai, H. Uehara, and H. Sakuma, 2008: An eddy-resolving hindcast simulation of the quasiglobal ocean from 1950 to 2003 on the Earth Simulator. *High Resolution Numerical Modelling of the Atmosphere and Ocean*, K. Hamilton and W. Ohfuchi, Eds., Springer, 157–185.

Treguier, A. M., and J. C. McWilliams, 1990: Topographic influences on wind-driven, stratified flow in a beta-plane channel: An idealized model for the Antarctic Circumpolar Current. *J. Phys. Oceanogr.*, 20, 321–343.

Tsujino, H., S. Nishikawa, K. Sakamoto, N. Usui, H. Nakano, and G. Yamanaka, 2013: Effects of large-scale wind on the Kuroshio path south of Japan in a 60-year historical OGCM simulation. *Clim. Dyn.*, 41, 2287–2318.

An Extra Product of the JRA-55 Atmospheric Reanalysis and In Situ Observations in the Kuroshio-Oyashio Extension Under the Japanese “Hotspot Project”

Hisashi Nakamura^{1,2}, Yoshimi Kawai²,
Ryusuke Masunaga¹, Hirotaka
Kamahori³, Chiaki Kobayashi³ and
Makoto Koike⁴

1. Research Center for Advanced Science and Technology, The University of Tokyo
2. Japan Agency for Marine-Earth Science and Technology, Yokohama, Japan
3. Meteorological Research Institute, Japan Meteorological Agency, Tsukuba, Japan
4. Department of Earth and Planetary Science, The University of Tokyo, Tokyo, Japan

Introduction

It is well established that the extratropical ocean tends to respond passively to mechanical and thermal forcing by the variability in the overlying atmosphere generated locally by internal dynamics or remotely through atmospheric teleconnection from the Tropics. Basin-scale atmospheric anomalies are maintained under the feedback forcing by synoptic-scale cyclones and anticyclones that recurrently develop along an oceanic stormtrack. The associated anomalous surface winds drive basin-scale anomalies in sea-surface temperature (SST) by modulating surface latent and sensible heat fluxes (hereafter LHF and SHF, respectively) and/or entrainment at the mixed-layer bottom. Over the North Pacific, the El Niño/Southern Oscillation (ENSO) leaves distinct imprints on SST by remotely modulating the stormtrack activity as “atmospheric bridge” (e.g., Alexander et al. 2002). During an El Niño event, for example, stronger surface westerlies yield negative SST anomalies over the central Pacific due to enhanced entrainment and heat release into the atmosphere.

Nevertheless, the passiveness of the extratropical ocean sounds rather counterintuitive if a climatic role of subtropical ocean gyres is considered in carrying a huge amount of heat from the Tropics. The transported heat is then released into the midlatitude atmosphere through LHF and SHF intensively from narrow western boundary currents (WBCs), including the Kuroshio. Under the strong influence of the East Asian winter monsoon, the Kuroshio, its eastward Extension and the Tsushima Current climatologically release as much as 2PW of sensible and latent heat into the atmosphere in January (Nakamura et al. 2015), which is twice as much as from the Gulf Stream (0.9PW), exerting thermodynamic forcing on the overlying atmosphere (Kelly et al. 2010; Kwon et al. 2010). Thus the western North Pacific, including the adjacent marginal seas, can be recognized as the most pronounced climatic “hot spot” among the global WBCs (Nakamura et al. 2015). This maritime domain is also characterized by the Subarctic Frontal Zone (SAFZ) in the Kuroshio-Oyashio Extension (KOE), a prominent oceanic frontal zone with strong SST gradient that is influential on the stormtrack formation (Nakamura et al. 2004). Persistent SST anomalies generated by decadal-scale SAFZ variability can force basin-scale atmospheric anomalies, with the anomalous surface Aleutian Low, by modulating stormtrack activity (Frankignoul et al. 2011; Taguchi et al. 2012). Aiming at deepening our understanding of oceanic and atmospheric processes occurring along the Kuroshio, in the KOE region and East Asian marginal seas, a project “Multi-Scale Air-Sea Interaction under the East-Asian Monsoon: A ‘Hot Spot’ in the Climate System” was funded from summer 2010 to spring 2015 by the Japanese Ministry of Education, Culture, Sports, Science and Technology (Nakamura et al. 2015). In this so-called “Hotspot project”, a total of a hundred scientists and graduate students from both the Oceanography and Meteorological Societies of Japan participated. By unifying advanced high-resolution numerical modeling on the Earth Simulator and new-generation satellite data and by conducting in situ observation campaigns, the project contributed substantially to deepening our understanding of multi-scale interactive processes involved actively in the air-sea heat and freshwater exchanges and their influence on the climate variability. In the following, two data sets as main outcomes from the project are introduced to the community.

Extra product of the Japanese reanalysis of the global atmosphere

Wide spectrum of multi-scale air-sea interaction within the “hot spots” has been revealed in recent satellite data and high-resolution numerical modeling. For example, satellite scatterometer measurements have revealed mesoscale patterns of surface wind convergence/divergence generated under the background winds blowing across frontal SST gradient (Xie 2004; Chelton et al. 2004; O’Neill 2010). On the warmer side of a SST front along a warm WBC, turbulent mixing of wind momentum is enhanced, and cross-frontal winds therefore act to generate surface convergence or divergence. Enhancement and suppression of heat release from the ocean on the warmer and cooler sides of the SST front also yield surface convergence and divergence, respectively, through hydrostatically lowering and raising surface pressure (Small et al. 2008; Shimada and Minobe 2011; Tanimoto et al. 2011). The surface convergence thus generated yields ascending motion at the top of the boundary layer, acting to enhance cloudiness and precipitation locally, for example, along the warm KE in winter (Tokinaga et al. 2009; Masunaga et al. 2015). Particularly high SST along the Kuroshio in the East China Sea can develop deep convective clouds, especially under the warm, moist monsoonal airflow from the Tropics (Sasaki et al. 2012; Miyama et al. 2012). In situ observations can barely identify the climatological signatures or snapshots

of these mesoscale atmospheric imprints of the Kuroshio and KE (Tokinaga et al. 2009; Tanimoto et al. 2011), but the spatial and temporal resolutions of the data are too coarse to investigate the variability of those imprints.

For this purpose a long-term atmospheric reanalysis dataset may be suited. However, its usefulness depends critically on the resolution not only for the forecast model used for data assimilation but also for the SST data used as the model lower-boundary condition. In this regard, the ERA-Interim (Dee et al. 2011) is unique, in which the resolution of the SST data used has been improved at the beginning of 2002. Masunaga et al. (2015, 2016a,b) have recently pointed out that those mesoscale atmospheric imprints of the KE as mentioned above are well represented climatologically in the ERA-Interim only in the period since 2002 and so are their modulations forced by the KE variability, while the corresponding imprints are virtually missing before 2002. Their findings indicate that circulation and thermal structure in the boundary layer is not strongly constrained by observations and their representation in reanalysis (or operational analysis) can therefore be highly sensitive to SST data prescribed in data assimilation.

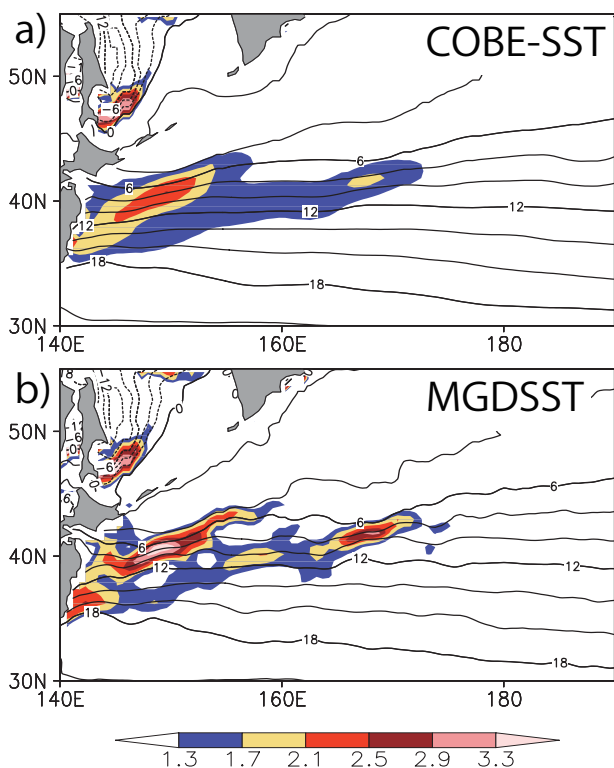


Figure 1: Climatological wintertime (DJFM) SST (every 2°C) over the North Pacific based on (a) COBE-SST and (b) MGDSSST. Climatological SST gradient (°C/100km) is colored. The climatology is defined for the period from 1985 to 2010 except for 1999-2003, in which JRA-55CHS is missing.

Motivated by Masunaga et al. (2015, 2016a,b), the Meteorological Research Institute (MRI) and University of Tokyo are now jointly preparing an extra product of a new Japanese reanalysis of the global atmosphere (JRA-55). As described in Kobayashi et al. (2015), the main product of JRA-55 has been produced for the period since 1958 with a state-of-the-art forecast model on T319 spectrum resolution (equivalent to ~60 km resolution) with 60 vertical levels, in which both satellite and other conventional measurements (e.g., radiosonde data) were assimilated through the 4DVAR method. As the lower-boundary condition for the JRA-55 main product, the COBE SST data set (Ishii et al. 2005) was used for the consistency over the entire data period. Based only on in situ observations, COBE SST is archived on 1-degree

resolution, which is coarser than that of the forecast model and insufficient for representing fine-scale SST structure (Fig. 1a). In contrast, the extra product under construction, called JRA-55CHS, utilizes the satellite-based MGDSSST data in place of COBE-SST used for the main product (“C” of JRA-55C and JRA-55CHS stands for “Conventional”, whereas “HS” for “High-resolution SST” and “Hot Spot”). The resolution of MGDSSST is quarter degree, which is sufficient for representing frontal SST gradient associated, for example, with the KE (Fig. 1b). Due to the limited availability of the MGDSSST data, JRA-55CHS, when completed, will become available for the period since 1982. Unlike in the main JRA-55 product, no satellite data for atmospheric variables are assimilated into JRA-55CHS due to the availability of computational

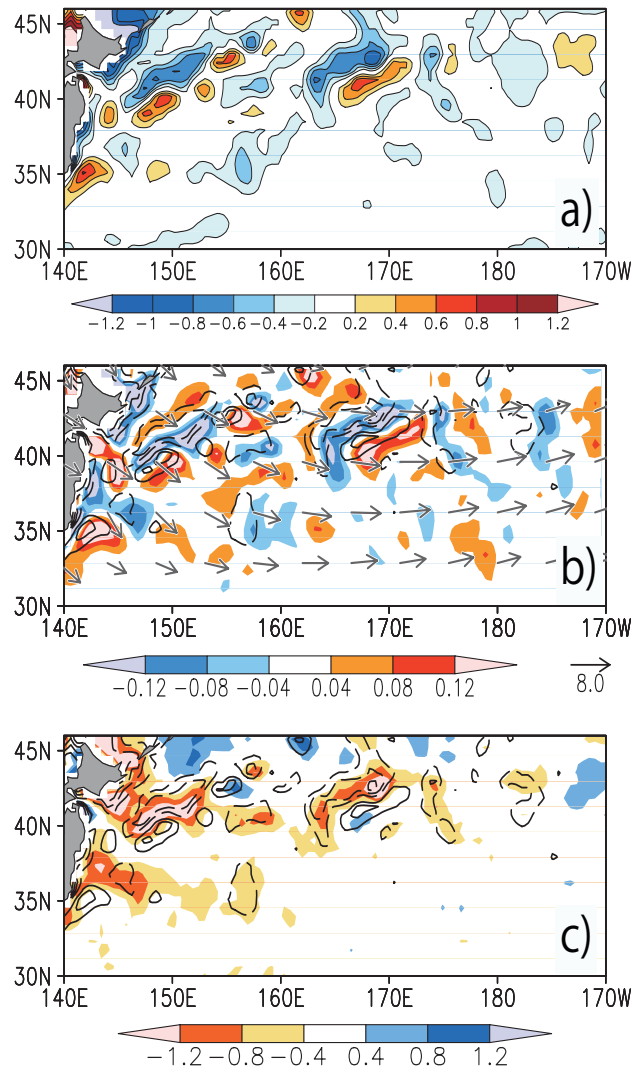


Figure 2: (a) Wintertime (DJFM) climatologies in MGDSSST over the North Pacific represented as local deviations (°C) from COBE-SST. (b) As in (a), but for surface wind convergence (positive) /divergence (negative) (10^{-5} s^{-1}) represented in JRA-55CHS as local deviations from that in JRA-55C. The SST difference shown in (a) is superimposed with contours (every 0.3°C; dashed for negative), and climatological surface winds in JRA-55CHS are plotted with arrows. (c) As in (b), but for total cloudiness (%). The climatology is defined for the period from 1985 to 2010 except for 1999-2003, in which JRA-55CHS is missing.

resource. In this regard, JRA-55CHS can be compared in a more straightforward manner with JRA-55C, another JRA-55 product that has been produced for the period since 1958 in the same manner as the main product but without satellite data.

Figure 2a shows a difference map of climatological SST for winter (December through March) between JRA-55CHS and

JRA-55C. Elongated dipolar SST differences apparent in Fig. 2a correspond to local SST fronts in the KOE region (Kida et al. 2015), which are better represented in MGDSSST for JRA-55CHS than in COBE-SST for JRA-55C (Fig. 1). Relative to JRA-55C, upward SHF in JRA-55CHS is locally enhanced and suppressed on the warmer and cooler sides, respectively, of each of those SST fronts, and so is upward LHF (not shown). Compared to JRA-55C, JRA-55CHS features mesoscale patterns of anomalous convergence/ divergence that correspond to enhanced frontal SST gradient in MGDSSST (Fig. 2b). As a local response to enhanced SST gradient, both the vertical mixing and hydrostatic pressure adjustment mechanisms seem operative to yield the anomalous convergence/divergence. Specifically, convergence is locally enhanced right over the warm KE just off the east coast of Japan, indicative of the dominant contribution from the pressure adjustment mechanism. Otherwise, the signatures of anomalous convergence/divergence appear to be displaced systematically from the local SST anomalies but collocated with the individual SST fronts that exhibit SW-NE tilts. This is an indication of the vertical mixing mechanism acting on the monsoonal northwesterlies. Crossing the fronts from their cooler to warmer sides, the surface northwesterlies tend to be accelerated by enhanced momentum mixing, yielding divergence along the fronts. Likewise, the enhanced momentum mixing over the warmer side of each of the SST fronts yields anomalous wind to its downstream relative in JRA-55CHS compared to JRA-55C. As evident in Fig. 2c, the climatological convergence and divergence signatures tend to accompany local increase and reduction, respectively, in cloudiness in a manner consistent with local vertical motion. Correspondingly, convective precipitation also tends to be modulated in JRA-55CHS. Note that the main JRA55 product exhibits almost the same characteristics as the JRA55C over the western North Pacific.

The aforementioned climatological local features of surface wind convergence/divergence and associated cloudiness represented in JRA-55C and JRA-55CHS (Fig. 2) overall resemble those in ERA-Interim for the periods before and after the beginning of 2002, respectively, and those features in JRA-55CHS are more consistent with satellite observations. Furthermore, our preliminary analysis shows that JRA-55CHS can reproduce enhancement of cloudiness and precipitation in the mixed-water region east of Japan during the unstable regime of the KE jet relative to its stable regime (c.f. Qiu and Chen 2005), as captured by satellite observations and by

ERA-Interim but only after 2001 (Masunaga et al. 2016a,b). The enhancement is an atmospheric response to augmented heat/moisture release from the warmer ocean with more active warm-core eddies (Sugimoto and Hanawa 2011).

In situ observations

Though recently acknowledged as powerful means of studying extratropical air-sea interactions, high-resolution numerical modeling and satellite observations still involve some uncertainties in simulating or measuring boundary-layer processes. Furthermore, their spatial and temporal resolutions are still insufficient for fully capturing variability of multi-scale phenomena involved in the air-sea interactions. For further improvement of numerical modeling and satellite observations, in situ observations are useful as benchmarks for model simulations and ground truth for satellite retrieval. In situ observations were conducted as a key activity of the “Hotspot project”, as introduced below.

One of the unique in situ observations by the “Hotspot project” was the deployment of a new mooring buoy near the KE for eight months from June 2012 (Fig. 3a), as an addition to two moored buoy sites within the KOE region: the Kuroshio Extension Observatory (KEO) and Japanese KEO (JKEO), situated to the south and north of the KE axis, respectively. The KEO buoy at 32.3°N, 144.6°E has been operative since 2004 by the U.S. NOAA/PMEL, whereas the JKEO buoy was operated at 38.0°N, 146.5°E from 2007 to 2013 by the Japan Agency for Marine-Earth Science and Technology Japan (JAMSTEC). The New KEO (NKEO) site at 33.8°N, 144.9°E for the extra buoy deployed was located between the KEO and JKEO sites, so as to monitor the meridional distribution of surface air pressure, SHF and LHF across the SST front along the KE. In reality, however, the KE axis just east of Japan was displaced anomalously northward in 2012, the SST difference between the KEO and NKEO sites was less than 2°C throughout the observation period. Furthermore, only a limited number of meteorological variables had been monitored since September 2012, when many meteorological sensors, including wind gauges, failed at both the JKEO and NKEO sites, probably due to contacts with fishing gear or vandalism. Still, SST and surface wind data obtained at the three buoys were utilized for the validation of AMSR2 onboard the GCOM-W satellite (Tomita et al. 2015). Furthermore, optical dissolved oxygen (DO) sensors installed on the mooring line of the NKEO buoy at 200, 400 and 600 m depths were successful in capturing DO changes in the subtropical mode water (STMW) and intrusions of oxygen-rich

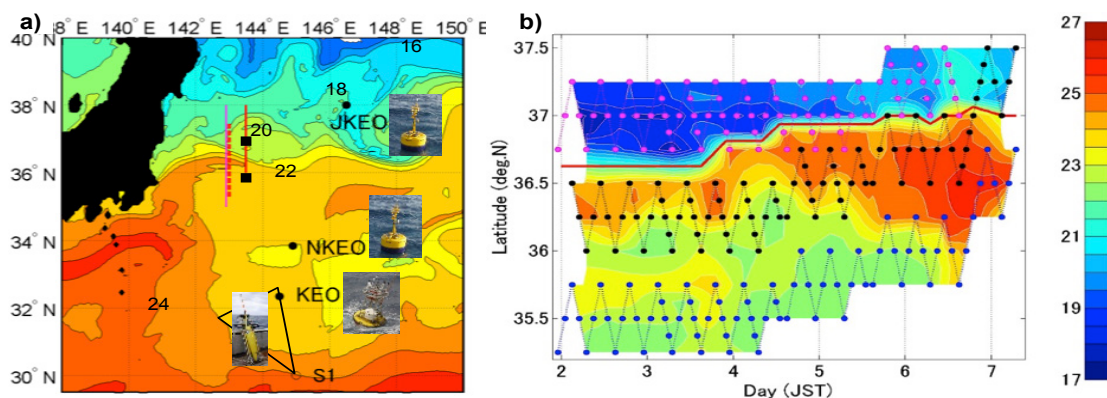


Figure 3: (a) JKEO, NKEO and KEO buoy sites (dots), superimposed on map of JCOPE2 SST on 2 July 2012 (colored; every 1 °C). The R/V Natsushima cruise in June 2012 and the coordinated three-vessel cruises in July 2012 were carried out along the pink solid and red dashed lines, respectively across the KE front. The R/V Kaiyo cruise in July 2013 was carried out along the red solid line jointly with aircraft observations whose sites are plotted with the closed squares. Triangular domain roughly defines the SeaGlider observation area. (b) Time-latitude section of SST observed in July 2012 by the three vessels (°C, colored) at 143°E along the red dashed line in (a), where the observed SST values were resampled hourly and then interpolated temporally and spatially. Red line represents the SST front. Dotted lines and dots denote the positions of the vessels and radiosonde observations, respectively. Seisui-maru (magenta) departed right after the observation at 1500 JST on 6 July, while R/V Wakataka-maru (black) and R/V Tansei-maru (blue) continued observations until 0700 JST on 7 July. After Kawai et al. (2015).

water underneath (Nagano et al. 2016). In addition, a GPS wave gauge installed on top of the NKEO buoy was also successful in monitoring wave height over eight months (Waseda et al. 2014). In spring of 2014, SeaGlider observations were carried out between the KE0 and S1 (30°N, 145°E) sites (Fig. 3a), to measure vertical profiles of temperature, salinity and DO.

Another unique in situ observations by the “Hotspot project” include an intensive observational campaign carried out in early 2012, which was characterized by three-vessel cruises across the KE front (Kawai et al. 2015). The three vessels, R/V Seisui-maru, R/V Wakataka-maru and R/V Tansei-maru, were aligned at latitudinal intervals of 30' or 45' along the 143°E meridian, moving back and forth meridionally within a half-degree section across the KE front (Fig. 3b) in launching radiosonde simultaneously every two hours. This formation was designed to overcome the particular difficulty the preceding single-vessel cruises encountered (Tanimoto et al. 2009; Tokinaga et al. 2009; Kawai et al. 2014) in attempting to identify impacts of the KE front on the atmosphere. Unlike those single-vessel cruises through which no complete separation is possible between spatial and temporal variations of the impacts, the three-vessel cruise made an atmospheric section across the KE front available every four hours throughout the 4-day period from 2 July (Kawai et al. 2015). During that period the KE front with marked SST contrasts displaced northward by about 50 km (Fig. 3b), which was not well represented in any of the objectively analyzed SST data sets available. As documented in more detail by Kawai et al. (2015), the observations captured cross-frontal differences in the mesoscale boundary-layer structure and their temporal modulations due to the passage of cyclones along the Baiu front. The bases of low-level clouds tended to be elevated over the warmer KE water due to enhanced turbulence activity within the developed mixed layer, and this cross-frontal contrast became particularly prominent under the near-surface northerlies. Likewise, joint observations with an aircraft and R/V Kaiyo were carried out north of the KE twice in July 2013 (Fig. 3a), in an attempt to detect possible modulations of the indirect aerosol effect on low-level clouds by the underlying SST. In spite of low cloudiness around the targeted area, the relationship between air-sea temperature difference and the ratio of cloud droplet number concentration to aerosol number concentration based on the particular observations for summertime water clouds near the KE seems consistent with the corresponding relationship obtained by Koike et al. (2012) for water clouds observed over the East China Sea in early spring. Furthermore, an aerosol-rich air mass in the free troposphere originating from the Asian continent seemed to be entrained into the mixed layer developing over the warm KE.

Concluding remarks

The “Hotspot project” was completed successfully with strong support from the international community. Most of those data produced and obtained through the project will become available for the community near future. The production of the JRA-55CHS data is under way and may become available sometime in 2017. Comparison of JRA-55CHS with JRA-55C, which is open to the community, will be useful for assessing impacts of the WBCs and associated SST fronts on the atmosphere. Since no satellite data are assimilated into either JRA-55CHS or JRA-55C, however, their reproducibility for the Southern Hemisphere is likely to be lower than that of ERA-Interim. Most of the in situ observation data obtained during the HotSpot project, including the NKEO buoy data, will be released at the Hot Spot website (<http://hadley1.atmos.rcast.u-tokyo.ac.jp/hotspot>), except the aircraft and SeaGlider data. A full list of datasets available has been compiled by Cronin (2016).

Acknowledgments

The “Hotspot project” was conducted under the support of the Japanese Ministry of Education, Culture, Sports, Science and Technology through the Grants-in-Aid for Scientific Research in Innovative Areas 2205. The aircraft observations were supported also by Grant-in-Aid for Scientific Research (A) 26241003.

References

- Alexander, M., I. Bladé, M. Newman, J. R. Lanzante, N.-C. Lau, and J. D. Scott, 2002: The atmospheric bridge: The influence of ENSO teleconnections on air–sea interaction over the global oceans. *J. Climate*, 15, 2205–2231.
- Chelton, D. B., M. G. Schlax, M. H. Freilich, and R. F. Milliff, 2004: Satellite measurements reveal persistent small-scale features in ocean winds. *Science*, 303, 978–983.
- Cronin, M. F., 2016: Where’s the Data? CLIVAR Exchanges 69 [this issue]
- Dee, D. P., and coauthors, 2011: The ERA-Interim reanalysis: configuration and performance of the data assimilation system. *Quart. J. Roy. Meteor. Soc.*, 137, 553–597.
- Frankignoul, C., N. Sennechael, Y.-O. Kwon, and M. A. Alexander, 2011: Influence of the meridional shifts of the Kuroshio and the Oyashio Extensions on the atmospheric circulation. *J. Climate*, 24, 762–777.
- Hotta D, Nakamura H (2011) On the significance of sensible heat supply from the ocean in the maintenance of mean baroclinicity along storm tracks. *J. Climate*, 24, 3377-3401.
- Ishii, M., A. Shouji, S. Sugimoto, and T. Matsumoto, 2005: Objective analyses of sea-surface temperature and marine meteorological variables for the 20th century using ICOADS and the Kobe Collection. *Int. J. Climatol.*, 25, 865-879.
- Kawai, Y., H. Tomita, M. F. Cronin, and N. A. Bond, 2014: Atmospheric pressure response to mesoscale sea surface temperature variations in the Kuroshio Extension: In situ evidence. *J. Geophys. Res. Atmos.*, 119, 8015-8031.
- Kawai, Y., T. Miyama, S. Iizuka, A. Manda, M. K. Yoshioka, S. Katagiri, Y. Tachibana, and H. Nakamura, 2015: Marine atmospheric boundary layer and low-level cloud responses to the Kuroshio Extension front in the early summer of 2012: Three-vessel simultaneous observations and numerical simulations. *J. Oceanogr.*, 71, 511-526.
- Kelly, K. A., R. J. Small, R. M. Samelson, B. Qiu, T. M. Joyce, Y.-O. Kwon, and M. F. Cronin, 2010: Western boundary currents and frontal air-sea interaction: Gulf Stream and Kuroshio Extension. *J. Climate*, 23, 5644-5667.
- Kida, S., and co-authors, 2015: Oceanic fronts and jets around Japan - a review. *J. Oceanogr.*, 71, 469-497.
- Koike, M., N. Takegawa, N. Moteki, Y. Kondo, H. Nakamura, K. Kita, H. Matsui, N. Oshima, M. Kajino, and T. Y. Nakajima, 2012: Measurements of regional-scale aerosol impacts on cloud microphysics over the East China Sea: Possible influences of warm sea surface temperature over the Kuroshio ocean current. *J. Geophys. Res. Atmos.*, 117, D17205.
- Kwon, Y.-O., M. A. Alexander, N. A. Bond, C. Frankignoul, H. Nakamura, B. Qiu, and L. Thompson, 2010: Role of Gulf Stream and Kuroshio-Oyashio systems in large-scale atmosphere-ocean interaction: A review. *J. Climate*, 23, 3249-3281.

- Masunaga, R., H. Nakamura, T. Miyasaka, K. Nishii K, and Y. Tanimoto, 2015: Separation of climatological imprints of the Kuroshio Extension and Oyashio fronts on the wintertime atmospheric boundary layer: Their sensitivity to SST resolution prescribed for atmospheric reanalysis. *J. Climate*, 1764-1787.
- Masunaga, R., H. Nakamura, T. Miyasaka, K. Nishii K, and B. Qiu, 2016a: Interannual modulations of oceanic imprints on the wintertime atmospheric boundary layer under the changing dynamical regimes of the Kuroshio Extension. *J. Climate*, 29, 3273-3296.
- Masunaga, R., H. Nakamura, T. Miyasaka, K. Nishii K, Y. Tanimoto, and B. Qiu, 2016b: Mesoscale imprints of the Kuroshio Extension and Oyashio Fronts on the wintertime atmospheric boundary layer. *CLIVAR Exchanges* (this volume).
- Miyama, M., M. Nonaka, H. Nakamura, and A. Kuwano-Yoshida, 2012: A striking early-summer event of a convective rainband persistent along the warm Kuroshio in the East China Sea. *Tellus*, A64, 18962
- Nakamura, H., T. Sampe, Y. Tanimoto, and A. Shimpo, 2004: Observed associations among storm tracks, jet streams and midlatitude oceanic fronts. "Earth's Climate: The Ocean-Atmosphere Interaction", *AGU Geophys. Monogr.*, 147, 329-346.
- Nakamura, H., A. Isobe, S. Minobe, H. Mitsudera, M. Nonaka, and T. Suga, 2015: "Hot spots" in the climate system – New developments in the extratropical ocean-atmosphere interaction research –: A short review and an introduction. *J. Oceanogr.*, 71, 463-467.
- Nagano, A., T. Suga, Y. Kawai, M. Wakita, K. Uehara, and K. Taniguchi, 2016: Ventilation revealed by the observation of dissolved oxygen concentration south of the Kuroshio Extension during 2012-2013. *J. Oceanogr.*, 72, in press.
- O'Neill, L. W., S. K. Esbensen, N. Thum, R. M. Samelson, and D. B. Chelton, 2010: Dynamical analysis of the boundary layer and surface wind responses to mesoscale SST perturbations. *J. Climate*, 23, 559-581.
- Qiu, B., and S. Chen, 2005: Variability of the Kuroshio Extension jet, recirculation gyre, and mesoscale eddies on decadal time scales. *J. Phys. Oceanogr.*, 35, 2090–2103.
- Sasaki, Y. N., S. Minobe, T. Asai, and M. Inatsu, 2012: Influence of the Kuroshio in the East China Sea on the early summer (Baiu) rain. *J. Climate*, 25, 6627-6645.
- Schneider N, Qiu B (2015) The atmospheric response to weak sea surface temperature fronts. *J Atmos Sci* 72. in press.
- Shimada, T., and S. Minobe, 2011: Global analysis of the pressure adjustment mechanism over sea surface temperature fronts using AIRS/Aqua data. *Geophys. Res. Lett.*, 38, L06704.
- Small, R. J., S. P. deSzoeke, S.-P. Xie, L. W. O'Neill, H. Seo, Q. Song, P. Cornillon, M. Spall, and S. Minobe, 2008: Air–sea interaction over ocean fronts and eddies. *Dyn. Atmos. Ocean*, 45, 274-319.
- Sugimoto, S., and K. Hanawa, 2011: Roles of SST anomalies on the wintertime turbulent heat fluxes in the Kuroshio-Oyashio Confluence Region: Influences of warm eddies detached from the Kuroshio Extension. *J. Climate*, 24, 6551-6561.
- Taguchi, B., H. Nakamura, M. Nonaka, N. Komori, A. Kuwano-Yoshida, K. Takaya, and A. Goto, 2012: Seasonal evolutions of atmospheric response to decadal SST anomalies in the North Pacific subarctic frontal zone: Observations and a coupled model simulation. *J. Climate*, 25, 111-139.
- Tanimoto, Y., T. Kanenari, H. Tokinaga, and S.-P. Xie, 2011: Sea level pressure minimum along the Kuroshio and its Extension. *J. Climate*, 24, 4419-4433.
- Tokinaga, H., Y. Tanimoto, S.-P. Xie, T. Sampe, H. Tomita, and H. Ichikawa, 2009: Ocean frontal effects on the vertical development of clouds over the western North Pacific: In situ and satellite observations. *J. Climate*, 22, 4241–4260.
- Wu L, Cai W, Zhang L, Nakamura H, Timmermann A, Joyce T, McPhaden MJ, Alexander MA, Qiu B, Visbeck M, Chang P, Giese B (2012) Enhanced warming over the global subtropical western boundary currents. *Nature Clim Change* 2. 161-166
- Xie, S.-P., 2004: Satellite observations of cool ocean-atmosphere interaction. *Bull. Amer. Meteor. Soc.*, 85, 195-208.

Mesoscale Imprints of the Kuroshio Extension and Oyashio Fronts on the Wintertime Atmospheric Boundary Layer

Ryusuke Masunaga¹, Hisashi Nakamura¹, Takafumi Miyasaka¹, Kazuaki Nishii¹, Youichi Tanimoto², Bo Qiu³

1. Research Center for Advanced Science and Technology, The University of Tokyo, Japan
2. Faculty of Environmental Earth Science, and Graduate School of Environmental Science, Hokkaido University, Sapporo, Japan
3. Department of Oceanography, University of Hawai'i at Mānoa, Honolulu, HI, USA

Introduction

In the Kuroshio-Oyashio Extension (KOE) region east of Japan, also known as the subarctic oceanic frontal zone (SAFZ), part of the cool Oyashio water flows southward along the east coast of Japan, while the rest flows eastward to the north of the Kuroshio Extension (KE), forming the mixed water region in between (Kawai 1972; Yasuda 2003; Kida et al. 2015). In the SAFZ, turbulent heat fluxes from the ocean are substantially enhanced in the cold season under dry, cold continental air mass advected by the prevailing monsoonal northerlies (e.g., Kwon et al. 2010). Despite a huge amount of heat release into the atmosphere, SST remains relatively high in winter along the KE owing to its advective effect. The SAFZ is recognized as one of the major centres of action of decadal sea surface temperature (SST) variability (Nakamura et al. 1997; Seager et al. 2001; Nakamura and Kazmin 2003). The decadal SST anomalies in the SAFZ can significantly modify the basin-scale atmospheric circulation by modulating stormtrack activity (e.g., Taguchi et al. 2012). Recent studies have revealed that locally enhanced turbulent heat fluxes due to warm SST can organize mesoscale structures climatologically in the marine atmospheric boundary layer (MABL), which cannot arise solely from atmospheric processes (e.g., Xie 2004; Small et al. 2008; Kelly et al. 2010). Locally warm SST can reduce static stability, where the turbulent “vertical mixing effect” enhances downward transport of wind momentum to locally accelerate sea-surface winds (Wallace et al. 1989), modulating sea-

surface wind divergence and curl (e.g., Nonaka and Xie 2003; Chelton et al. 2004). At the same time, local SST maxima/minima modulate heat fluxes into the overlying atmosphere, leading to the formation of local minima/maxima of sea-level pressure (SLP) through “hydrostatic effect” (Lindzen and Nigam 1987). In fact, Tanimoto et al. (2011) found a distinct SLP trough along the KE in a long-term ship-measured climatology in winter, which leads to local enhancement of cloud formation and precipitation (Tokinaga et al. 2009; Minobe et al. 2010). Tanimoto et al. (2011) also argued that a combination of “hydrostatic effect” and “vertical mixing effect” climatologically yields a characteristic distribution of near-surface ageostrophic winds around the KE.

It has been pointed out that the KE fluctuates between its stable and unstable regimes on (quasi-) decadal time scales (e.g., Qiu and Chen 2005). In its unstable regime, eastward transport of the KE decreases and its path tends to be more meandering, while its stable regime is characterized by the stronger KE jet with its more zonal path. Several studies have documented relationship between SST anomalies associated with the KE variability and local mesoscale MABL structures (Iizuka 2010; Wang and Liu 2016) or large-scale atmospheric circulation including the strength of the Aleutian low and storm track activity (e.g., Qiu et al. 2014; Révelard et al. 2016).

This short article is a summary of Masunaga et al. (2015, 2016), who investigated climatological mesoscale imprints of KE and Oyashio fronts on the wintertime MABL and their modulations associated with interannual- to decadal-scale KE variability.

Wintertime climatology

In the KOE region, part of the Oyashio flows eastward to the north of the KE in forming two distinct SST fronts, namely Oyashio and KE fronts (e.g., Nonaka et al. 2006), as captured by such high-resolution satellite SST data as OISST (Reynolds et al. 2007). To investigate mesoscale imprints of these two SST fronts on the overlying atmosphere, we utilize the ERA-Interim global atmospheric reanalysis (Dee et al. 2011), in which the resolution of prescribed SST data has been substantially improved since 2002. Specifically, the SST resolution is $1.0^\circ \times 1.0^\circ$ in January 1979 through December 2001, $0.5^\circ \times 0.5^\circ$ in January 2002 through January 2009, and $0.05^\circ \times 0.05^\circ$ since February 2009. We have confirmed that the latter improvement exerts virtually no impacts on the atmospheric fields represented in the forecast model with horizontal resolution of 0.75° . In the wintertime (December through March) climatology for the period from January 2002 through March 2014, the SST field prescribed for the ERA-Interim resolves the KE and Oyashio fronts separately as distinct dual peaks of SST gradient $|dSST/dy|$ (Fig. 1b), whereas the $|dSST/dy|$ exhibits a broad single maximum in its low-resolution SST period (1979 through 2001) (Fig. 1a). In the ERA-Interim in its high-resolution SST period, surface upward heat fluxes yield two local maxima on the warmer flanks of these oceanic fronts, and thereby overlying MABL is locally warmed, leading to dual local minima of SLP in its meridionally high-pass-filtered field (hereafter hSLP) through “hydrostatic effect”. Indeed, there are corresponding dual-peak profiles in surface wind convergence, upward motion and MABL depth. These mesoscale features are manifested as local maxima of total cloud amount (TCA) along both the KE and Oyashio fronts (Fig. 1d). Precipitation, especially convective rainfall, also exhibits local enhancement on the warmer flanks of these oceanic fronts. In the low-resolution SST period, by contrast, these mesoscale atmospheric features are totally missing in correspondence to artificially smoothed SST distribution, as represented in TCA fields (Fig. 1c). These results suggest that both the KE and Oyashio fronts

can climatologically leave mesoscale imprints on the MABL, leading to dual-peak profiles in mesoscale atmospheric fields.

Variability

To investigate how the mesoscale atmospheric features described above tend to be modulated due to the decadal-scale regime changes of the KE system (e.g., Qiu and Chen 2005), composite maps of wintertime SST and $|dSST/dy|$ prescribed for the ERA-Interim are constructed separately for the unstable and stable regimes based on the KE Index (KEI) defined by Qiu et al. (2014). Here, we focus on the period 2002-14, in which resolution of SST data prescribed for the ERA-Interim is high enough to represent the KE and Oyashio fronts. The KE front along 36°N is particularly distinct in its stable regime (colored in Fig. 2b), while it is substantially weaker in the unstable regime (colored in Figs. 2a). The composited difference in SST (Fig. 2c) indicates zonally elongated dipolar anomalies. In the unstable KE regime, more warm-core eddies are detached from the KE jet northward (Sugimoto and Hanawa 2011; Sasaki and Minobe 2015). Therefore SST is higher than normal to the north of the mean KE jet, and the Oyashio front located to the north tends to be stronger. Composites of wintertime TCA exhibit a distinct local maximum along the KE in stable KE regime (Fig. 2h), while TCA is higher broadly over the KOE region in the unstable regime (Fig. 2g). Their difference is characterized as a significant enhancement of TCA right over the mixed water region in unstable KE regime (Fig. 2i), which accompanies anomalous surface wind convergence (Fig. 2f). In fact, other atmospheric fields, including upward turbulent heat fluxes, meridionally high-pass-filtered SLP and virtual potential temperature within MABL, and convective precipitation indicate significant composited differences over the mixed water region. These results indicate that mesoscale atmospheric features as imprints of the KE front are modulated with SST variations associated with variability of KE system. Although most of the significant anomalies are confined to the MABL, significant anomalies in vertical motion are found to reach the 750-hPa level.

Furthermore, we have examined the longer-term SST variability using OISST data, which is available since 1982 winter. We found that the composited SST fields are similar to those in Fig. 2a-b since the late 1980s, namely anomalously warm SST localized over the mixed water region in the unstable KE regime, and vice versa. In the mid-1980s, however, SST is anomalously cool over the KOE region even though KE is in the unstable regime according to the KEI, owing to anomalously strong southward Oyashio current along the east coast of Japan (Nakamura and Kazmin 2003; Nonaka et al. 2006). In fact, Miyasaka et al. (2014) pointed out the change of dominant decadal-scale SST variability over the North Pacific region in the late 1980s. It remains to be examined how SST has been varying in accordance with the modulation of the KE and Oyashio current in inter-decadal time scales, for example, by using long-term hindcast run of eddy-resolving ocean general circulation models.

Mechanisms for surface wind modulations

Two major mechanisms have been proposed through which mesoscale SST anomalies modulate sea-surface wind fields, namely “hydrostatic effect” and “vertical mixing effect”. We have confirmed that the composited distributions of meridionally high-pass-filtered virtual air temperature and their difference within the MABL can well explain the composited hSLP anomalies through hydrostatic relationship. This result is indicative of the “hydrostatic effect” operative under the KE regime changes. In fact, the interannual correlation (-0.86) is significant between winter-mean anomalies in hSLP and surface wind convergence if averaged over the mixed water

region. We consider, however, that modulations in “vertical mixing effect” can also play an important role. Indeed, composited anomalous eastward SST gradient ($dSST/dx$) exhibits a nearly in-phase pattern with zonal component of anomalous surface wind divergence (du_x/dx). Furthermore, vertical wind shear in MABL over the mixed water region is significantly weakened in the unstable KE regime in association with anomalously warm SST (See Fig. 13 of Masunaga et al. 2016). These can be indicative of the “vertical mixing effect” operative (e.g., Hayes et al. 1989). Please refer to discussion in section 4c of Masunaga et al. (2016) for more detail.

It will be examined in future study how the relative importance between the two processes varies with the KE variability to modify near-surface wind distribution by using some diagnostics or idealized boundary layer models (e.g., Schneider and Qiu 2015).

Summary and discussion

On the basis of the ERA-Interim we investigated the wintertime mesoscale imprints of the KE and Oyashio fronts on the overlying atmosphere and how they are modulated associated with decadal-scale variability of the KE system. We have revealed that both KE and Oyashio fronts can climatologically leave mesoscale imprints on the overlying atmosphere, leading to dual-peak meridional profiles of surface heat fluxes, MABL temperature, ascent, surface wind convergence, TCA and convective precipitation over the KOE region. Furthermore, these mesoscale atmospheric features are significantly modulated by SST anomalies associated with the decadal-scale KE variability. These results have been verified by using high-resolution state-of-the-art satellite data available in this century including QuikSCAT for sea-surface wind, MODIS (Hubanks et al. 2008) for TCA and AMSR-E for total precipitation. These mesoscale atmospheric features are, however, totally missing in ERA-Interim in its low-resolution SST period. These results suggest the importance of high-resolution SST data for atmospheric reanalysis to improve their representation of mesoscale atmospheric fields. Therefore, in the future study, it will be meaningful to use additional products of the new Japanese reanalysis of the global atmosphere (JRA-

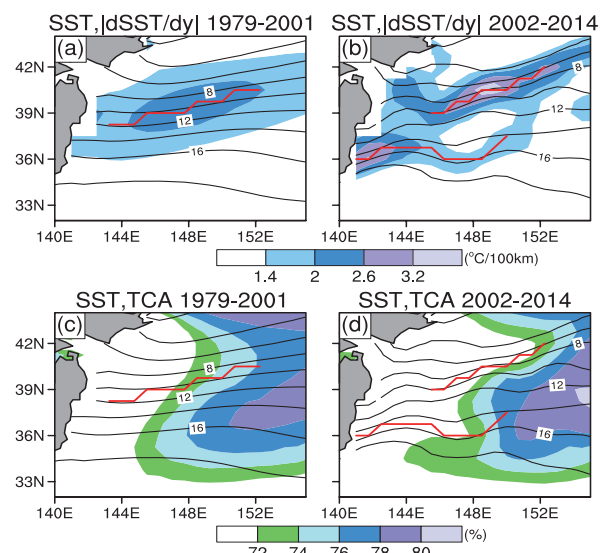


Figure 1: Climatological-mean wintertime (December-March) distributions of (a) SST (contoured for every 2°C) and its equatorward gradient ($|dSST/dy|$) [$^{\circ}\text{C} (100 \text{ km})^{-1}$; colored] based on the ERA-Interim from January 1979 through December 2001. (c) Same as in (a), but for total cloud amount (%) in place of $|dSST/dy|$. (b), (d) Same as in (a) and (c), respectively, but for the period from January 2002 through March 2014. Red lines indicate SST fronts at which climatological-mean $|dSST/dy|$ maximizes in each period.

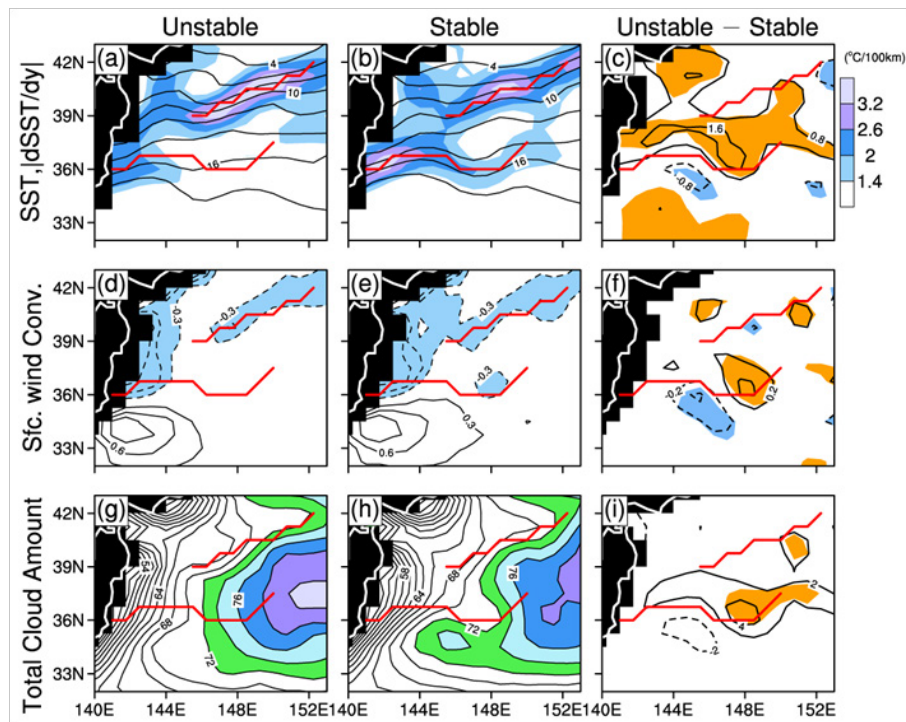


Figure 2: Wintertime SST (contoured for every 2°C) and its equatorward gradient ($|dSST/dy|$) [$^{\circ}\text{C}/(100\text{km})^2$]; shaded as indicated to the far right] composited for the (a) unstable and (b) stable regimes of KE on the basis of the Kuroshio Extension index. (c) Composite difference [(a) - (b)] of SST (contoured for every 0.8°C; zero contours are omitted). (d-e) Same as in (a-b), respectively, but for surface wind convergence (contoured for every $0.3 \times 10^{-5} \text{ s}^{-1}$; positive for convergence; shaded where its values are below $-0.3 \times 10^{-5} \text{ s}^{-1}$) and (f) their difference (contoured for every 0.2; zero contours are omitted). (g-h) Same as in (a-b), respectively, but for total cloud amount (contoured for every 2%; shaded where its values exceed 72%) and (i) their difference (contoured for every 2%; zero contours are omitted). Red lines indicate the KE and Oyashio fronts. Shadings are applied in (c), (f) and (i) where the difference is statistically significant at the 90% confidence level.

55; Kobayashi et al. 2015), in which high-resolution SST data ($0.25^{\circ} \times 0.25^{\circ}$) is used for data assimilation.

Acknowledgments

This study is supported in part by Japanese Ministry of Education, Culture, Sports Science and Technology (MEXT) through Grants-in-Aid for Scientific Research in 2205, 2409 (in Innovative Areas) and 25287120 and by the Japanese Ministry of Environment through the Environment Research and Technology Department Fund 2A1201 and 2-1503. BQ acknowledges support from NASA Grant NNX13AE51G.

References

Chelton, D. B., M. G. Schlax, M. H. Freilich, and R. F. Milliff, 2004: Satellite measurements reveal persistent small-scale features in ocean winds. *Science*, 303, 978–983.

Dee, D. P., and coauthors, 2011: The ERA-Interim reanalysis: configuration and performance of the data assimilation system. *Quart. J. Roy. Meteor. Soc.*, 137, 553–597.

Hayes, S. P., M. J. McPhaden, and J. M. Wallace, 1989: The influence of sea surface temperature on surface wind in the eastern equatorial Pacific: Weekly to monthly variability. *J. Climate*, 2, 1500–1506.

Hubanks, P. A., M. D. King, S. A. Platnick, and R. A. Pincus, 2008: MODIS Atmosphere L3 Gridded Product Algorithm Theoretical Basis Document. ATBD Reference Number ATBD-MOD-30, 96 pp. [Available online at http://modis-atmos.gsfc.nasa.gov/_docs/L3_ATBD_2008_12_04.pdf]

Iizuka, S., 2010: Simulations of wintertime precipitation in the vicinity of Japan: Sensitivity to fine-scale distributions of SST. *J. Geophys. Res.*, 117, D10107, doi:10.1029/2009JD012576.

Kawai, H., 1972: Hydrography of the Kuroshio Extension. *Kuroshio: Its Physical Aspects*, H. Stommel and K. Yoshida, Eds., University of Tokyo Press, 235–352.

Kelly, K. A., R. J. Small, R. M. Samelson, B. Qiu, T. M. Joyce, Y.-O. Kwon, and M. F. Cronin, 2010: Western boundary currents and frontal air-sea interaction: Gulf Stream and Kuroshio Extension. *J. Climate*, 23, 5644–5667.

Kida, S., and Coauthors, 2015: Oceanic fronts and jets around Japan: a review. *J. Oceanogr.*, 71, 469–497.

Kobayashi, S., and coauthors, 2015: The JRA-55 Reanalysis: general specifications and basic characteristics. *J. Meteor. Soc. Japan*, 93, 5–48.

Kwon, Y.-O., M. Alexander, N. Bond, C. Frankignoul, H. Nakamura, B. Qiu, and L. Thompson, 2010: Role of the Gulf Stream and Kuroshio-Oyashio systems in large-scale atmosphere-ocean interaction: A review. *J. Climate*, 23, 3249–3281.

Lindzen, R. S., and S. Nigam, 1987: On the role of sea surface temperature gradients in forcing low-level winds and convergence in the Tropics. *J. Atmos. Sci.*, 44, 2418–2436.

Masunaga, R., H. Nakamura, T. Miyasaka, K. Nishii and Y. Tanimoto, 2015: Separation of climatological imprints of the Kuroshio Extension and Oyashio fronts on the wintertime atmospheric boundary layer: Their sensitivity to SST resolution prescribed for atmospheric reanalysis. *J. Climate*, 28, 1764–1787.

Masunaga, R., H. Nakamura, T. Miyasaka, K. Nishii and B. Qiu, 2016: Interannual modulations of oceanic imprints on the wintertime atmospheric boundary layer under the changing dynamical regimes of the Kuroshio Extension. *J. Climate*, 29,

3273-3296.

Minobe, S., M. Miyashita, A. Kuwano-Yoshida, H. Tokinaga and S.-P. Xie, 2010: Atmospheric response to the Gulf Stream: seasonal variations. *J. Climate*, 23, 3699–3719.

Miyasaka, T., H. Nakamura, B. Taguchi, and M. Nonaka, 2014: Multidecadal modulations of the low-frequency climate variability in the wintertime North Pacific since 1950. *Geophys. Res. Lett.*, 41, 2948–2955.

Nakamura, H., G. Lim, and T. Yamagata, 1997: Decadal climate variability in the North Pacific during the recent decades. *Bull. Amer. Meteor. Soc.*, 78, 2215–2225.

Nakamura, H., and A. S. Kazmin, 2003: Decadal changes in the North Pacific oceanic frontal zones as revealed in ship and satellite observations. *J. Geophys. Res.*, 108, 3078-3094.

Nonaka, M., and S.-P. Xie, 2003: Covariations of sea surface temperature and wind over the Kuroshio and its extension: Evidence for ocean-to-atmosphere feedback. *J. Climate*, 16, 1404-1413.

Nonaka, M., H. Nakamura, Y. Tanimoto, T. Kagimoto, and H. Sasaki, 2006: Decadal variability in the Kuroshio-Oyashio Extension simulated in an eddy-resolving OGCM. *J. Climate*, 19, 1970–1989.

Qiu, B., and S. Chen, 2005: Variability of the Kuroshio Extension jet, recirculation gyre, and mesoscale eddies on decadal time scales. *J. Phys. Oceanogr.*, 35, 2090–2103.

Qiu, B., S. Chen, N. Schneider, and B. Taguchi, 2014: A coupled decadal prediction of the dynamic state of the Kuroshio Extension system. *J. Climate*, 27, 1751–1764.

Reynolds, R.W., T. M. Smith, C. Liu, D. B. Chelton, K. S. Casey, and M. G. Schlax, 2007: Daily high-resolution-blended analyses for sea surface temperature. *J. Climate*, 20, 5473–5496.

Révelard, A., C. Frankignoul, N. Sennéchaël, Y.-O. Kwon and B. Qiu, 2016: Influence of the decadal variability of the Kuroshio Extension on the atmospheric circulation in the cold season. *J. Climate*, 29, in press.

Sasaki, Y. N., and S. Minobe, 2015: Climatological mean features and interannual to decadal variability of ring formations in the Kuroshio Extension region. *J. Oceanogr.*, 71, 499–509.

Schneider, N., and B. Qiu, 2015: The atmospheric response to weak sea surface temperature fronts. *J. Atmos. Sci.*, 72, 3356–3377.

Seager, R., Y. Kushnir, N. H. Naik, M. A. Cane, and J. Miller, 2001: Wind-driven shifts in the latitude of the Kuroshio-Oyashio Extension and generation of SST anomalies on decadal timescales. *J. Climate*, 14, 4249–4265.

Small, R. J., and Coauthors, 2008: Air-sea interaction over ocean fronts and eddies. *Dyn. Atmos. Oceans*, 45, 274–319.

Sugimoto, S., and K. Hanawa, 2011: Roles of SST anomalies on the wintertime turbulent heat fluxes in the Kuroshio–Oyashio confluence region: Influences of warm eddies detached from the Kuroshio Extension. *J. Climate*, 24, 6551–6561.

Taguchi, B, H. Nakamura, M. Nonaka, N. Komori, A. Kuwano-Yoshida, K. Takaya, and A. Goto, 2012: Seasonal evolutions of

atmospheric response to decadal SST anomalies in the North Pacific subarctic frontal zone: Observations and a coupled model simulation. *J. Climate*, 25, 111–139.

Tanimoto, Y., T. Kanenari, H. Tokinaga, and S.-P. Xie, 2011: Sea level pressure minimum along the Kuroshio and its Extension. *J. Climate*, 24, 4419–4433.

Tokinaga, H., Y. Tanimoto, S.-P. Xie, T. Sampe, H. Tomita, and H. Ichikawa, 2009: Ocean frontal effects on the vertical development of clouds over the western North Pacific: In situ and satellite observations. *J. Climate*, 22, 4241–4260.

Wallace, J. M., T. P. Mitchell, and C. Deser, 1989: The influence of sea surface temperature on surface wind in the eastern equatorial Pacific: Seasonal and interannual variability. *J. Climate*, 2, 1492–1499.

Wang, Y., and T. Liu, 2016: Observational evidence of frontal-scale atmospheric responses to Kuroshio Extension variability. *J. Climate*, 29, in press.

Xie, S.-P., 2004: Satellite observations of cool ocean–atmosphere interaction. *Bull. Amer. Meteor. Soc.*, 85, 195–208.

Yasuda, I., 2003: Hydrographic structure and variability in the Kuroshio-Oyashio transition area. *J. Oceanogr.*, 59, 389–402.

Where's the Data?

Meghan F. Cronin

NOAA Pacific Marine Environmental Laboratory,
Seattle WA USA

Introduction

CLIVAR has a very clear data policy. All CLIVAR data should be made available freely and without restrictions, with minimal delay (preferably also in real-time). The details of the data policy can be found at:

<http://www.clivar.org/resources/data/data-policy>

In addition, many peer-reviewed journals are now instituting data policies requiring authors to show where to access all data (including from numerical models) used in the paper. For the American Geophysical Union policy, see:

<http://publications.agu.org/author-resource-center/publication-policies/data-policy/>. In general, an independent group should be able to access the data used in the study and replicate the results using the same data. Modellers also want to test the reproducibility of these observations and results in their numerical models.

So where are the data?

This question was asked at the recent CLIVAR-JAMSTEC Workshop on the Kuroshio Current and Extension System: Theory, Observations, and Ocean Climate Modelling, which was held jointly with the CLIVAR Ocean Model Development Panel meeting in Yokohama Japan. This article is an attempt at a fuller answer than the one provided at the workshop.

I shall begin by describing where my data from the Kuroshio Extension Observatory (KEO) can be accessed. I lead the NOAA Pacific Marine Environmental Laboratory (PMEL) Ocean Climate Stations (OCS) group, which maintains the NOAA KEO surface mooring in the recirculation gyre south of the Kuroshio Extension, and the NOAA Station Papa mooring in the NE Pacific subpolar gyre. The OCS webpages are rich in content, providing details about the moorings and sensors, the motivation and history of the sites, publication lists, and links to partner webpages and data sets. We have an easy to use data display and delivery page for the observations, as well as for air-sea fluxes computed from the data. Please explore our website: <http://www.pmel.noaa.gov/OCS/>

From 2007-2013, JAMSTEC had a surface mooring (JKEO) deployed north of the Kuroshio Extension (KE). KEO and JKEO data have been used to investigate how the KE affects the atmosphere through air-sea fluxes. JKEO data and metadata can be accessed through its project website: <http://www.jamstec.go.jp/iorgc/ocorp/ktsfg/data/jkeo/index.html>

Both KEO and JKEO are part of OceanSITES (<http://www.oceansites.org/>), a global network of long-term, deepwater reference stations that aim to provide full-water column, multi-disciplinary time series at fixed locations. As with other observational networks, OceanSITES provides one-stop shopping for accessing all station data within its network. In particular, OceanSITES data are served in a self-documented common format through two Global Data Assembly Centres (GDAC), which can be explored through a web interface: <http://dods.ndbc.noaa.gov/oceansites/> or through ftp (<ftp://ftp.ifremer.fr/ifremer/oceansites/>).

The KEO mooring was initiated during the Kuroshio Extension System Study (KESS), a process study, funded primarily by the US National Science Foundation (NSF), that took place between 2004 and 2006 with the objective of determining the processes governing the strength and structure of the Kuroshio Extension recirculation gyres in relation to the meandering jet. The KESS observational array included a line of tall profiling moorings, embedded in an array of 46 inverted echo sounders with bottom pressures and current meters (CPIES). These data, as well as the shipboard measurements, Argo float data, and KEO mooring data, are all available through the KESS website: <http://uskess.whoi.edu/>. As with KEO, the KESS Argo float data are available through the PI-maintained websites (e.g. <http://www.soest.hawaii.edu/sno1/>) and the Argo network website: <http://www.argo.ucsd.edu/index.html>.

From 2010 to 2014, the Japanese Hot-Spot in Climate System Experiment carried out intensive ocean and atmosphere observations to investigate how mid-latitude fronts associated with the KE system and with the land-sea boundary affected the climate system. Hot-Spot observations were made from nearly every type of platform (e.g., ships, moorings, aircraft, floats). These data are available through the JAMSTEC data portal: <http://www.godac.jamstec.go.jp/dataportal/viewer.htm>

For finding gridded data, including many satellite products, the Asia-Pacific Data-Research Center (APDRC) of the University of Hawaii International Pacific Research Center (IPRC) provides an excellent starting point. See: <http://apdrc.soest.hawaii.edu/>

While this answer is more full than the one provided at the CLIVAR workshop, it is not a comprehensive list. Rather it is intended as a helpful starting point -- a roadmap for finding data. Please explore! I hope this will spur further dialogue and collaborations.

Acknowledgements

This is PMEL contribution number 4456.

Summary of the 2nd Session of the CLIVAR Ocean Model Development Panel (OMDP) - Extended Meeting on Forcing Ocean-Ice Climate Models

Anna Pirani¹, Gokhan Danabasoglu²,
Simon Marsland³

1. Université Paris Saclay, Saint-Aubin, France and The Abdus Salam International Centre for Theoretical Physics, Trieste, Italy
2. National Center for Atmospheric Research (NCAR), Boulder, CO, USA
3. CSIRO Oceans and Atmosphere, Aspendale, Australia

Introduction

The 2nd Session of the CLIVAR Ocean Model Development Panel (OMDP) was held on 14-16 January 2016 at the Japan Agency for Marine-Earth Science and Technology (JAMSTEC) in Yokohama, Japan. OMDP is grateful for the organization of the logistical aspects of the meeting by Yoshiki Komuro. The meeting agenda, links to presentations, and further information are available on the meeting website at <http://www.clivar.org/omdp/japan2016>.

The meeting was an extended OMDP session, whereby the invitation to participate was extended to all those directly involved in the development of the Coordinated Ocean-ice Reference Experiments phase II (CORE-II) and the Ocean Model Intercomparison Project (OMIP) protocol as well as those who have been participating in CORE-II simulations and their analysis. Furthermore, participation was extended beyond those who could travel to Japan in person with a live streaming connection generously provided by the NOAA Modeling, Analysis, Predictions, and Projections Program.

The focus of the meeting was primarily on a detailed evaluation of the new Japanese Reanalysis (JRA-55) atmospheric product for forcing ocean – sea-ice climate models produced by the Japan Meteorological Agency (JMA). Presentations and discussions included technical aspects of the JRA-55 reanalysis, the JRA-55 / OMDP collaborative evaluation that has been on-going since early 2015, reviews of applied and /

or additional corrections; creation of a repeat-annual-cycle forcing data set; and preliminary simulations forced with the JRA-55 data sets. An important goal of the meeting was to receive input from the wider ocean and climate modelling communities participating in the CORE-II and OMIP efforts.

Forcing Ocean – Sea-ice Climate Models

The CORE framework was first introduced in Griffies et al. (2009). The framework defines protocols for performing global ocean – sea-ice coupled simulations forced with common atmospheric data sets. Therefore, the most essential element of the CORE framework is the forcing data sets, which were developed by Large and Yeager (2004; 2009). The overarching hypothesis of a CORE comparison project is that global ocean – sea-ice models run under the same atmospheric state produce qualitatively similar solutions. This hypothesis has been found to be valid for a certain phenomena / diagnostics, but invalid for many others. Manuscripts analyzing the solutions from the participating models have been published in a Special Issue of Ocean Modelling: www.sciencedirect.com/science/journal/14635003/vsi/10PSR6J3BV4.

To date, the CORE data sets and protocol have been collaboratively led and supported by NCAR and the NOAA Geophysical Fluid Dynamics Laboratory (GFDL) under the OMDP (and formerly WGOMD). While the success and visibility of the CORE effort have been steadily increasing, no significant new developments or maintenance of the data sets or the protocol have occurred during the last 5-6 years. Broad advances in ocean and climate science have highlighted a need to advance the scientific and engineering foundations of CORE.

To foster such progress, OMDP convened a mini-workshop on forcing ocean and sea-ice models in Grenoble, France on 29-30 January 2015 (ICPO, 2015). A major focus was a discussion of the state-of-the-art of various reanalysis products and efforts as well as of various surface flux data sets and satellite products (e.g., ERA, JRA-55, ECMWF, HOAPS, etc.). Following extensive discussions, a major outcome of the mini workshop was the evaluation of the JRA-55 reanalysis product compared to other products towards its adaption as the next generation of atmospheric forcing data sets for use in the future CORE frameworks. The JRA-55 data sets (Kobayashi et al. 2015) cover the period from 1958 to present, featuring both high spatial (TL319 grid) and temporal (3-hourly) resolutions. Furthermore, they will be updated on a near-real time basis. JRA-55 is the first comprehensive reanalysis that has covered the last half-century since ERA-40 by ECMWF, and is the first one to apply 4D-variational data assimilation to this period.

A JRA-55 / OMDP collaborative effort has been underway since early 2015 to evaluate the JRA-55 data set for use in forcing ocean – sea-ice models. The evaluation has indicated that JRA-55 requires adjustments (bias corrections) as done in CORE for NCEP/NCAR reanalysis and in DRAMM for ECMWF reanalyses, and tests have been undertaken on various adjustment methods. Preliminary comparisons with in-situ observations by buoys show that surface atmospheric elements of the adjusted data are generally improved compared with the JRA-55 raw data. Air temperature and specific humidity fields near coasts and islands are affected by observations on land which are included in the JRA-55 screen-level analysis, requiring further improvement in the adjustment method.

Several initial intercomparison efforts evaluating model solutions obtained with the new JRA-55 product vs. some other forcing data sets have been undertaken. These include: i) the JMA-MRI global model forced by different

development versions of JRA-55 and the CORE-II forcings; ii) Community Earth System Model (CESM) ocean and sea-ice component models forced with JRA-55, CORE-II, and the NOAA/CIRES 20th Century Reanalysis (Compo et al. 2011); iii) MOM simulations forced with JRA-55 and CORE-II; and iv) NEMO simulations forced with JRA-55 and DRAKKAR data sets. The OMDP meeting report (ICPO, 2016) provides more details on the evaluation and adjustment methods and reference datasets used.

Based on the outcomes of these evaluation efforts and after detailed discussions, OMDP endorsed the JRA-55 activity for the development of the next version of the OMIP experiment, while the current CORE-II forcing is used for the version of OMIP currently underway within the Coupled Model Intercomparison Project phase 6 (CMIP6) initiative. The JRA-55 / OMDP collaborative evaluation activity will continue to diagnose more comprehensively various issues identified in the evaluation so far, and explore how to further improve the application of JRA-55 to force ocean – sea-ice models. The distribution of the dataset once ready for public release will be done through PCMDI.

Advancing the CORE Protocol

Several aspects of the CORE protocol were reviewed. These were identified as items that could be improved, considering participants' experiences with the protocol over the past 5+ years. They include revisiting the normal year forcing objectives and expectations considering alternative strategies such as Repeat Annual Cycle Forcing and the approach developed by the DRAKKAR consortium. The sensitivity of CORE-II/OMIP simulations to the CORE-II/OMIP spin-up strategy will be revisited and tested.

In terms of salinity restoring, OMDP recommends the use of weak restoring as the preferred choice (e.g., with a cap of 0.5 psu). If models choose an alternative strategy, they should document the approach used. Recommendations are being developed on Greenland and Antarctic liquid and solid freshwater flux estimates for future versions of OMIP. OMDP also recommends that groups document how Mediterranean Outflow is treated, including its salinity properties and how the outflow water propagates in the North Atlantic.

A new CORE-II analysis was proposed to examine the role played by the ocean's meridional overturning circulation in the uptake and sequestration of transient tracers from the CMIP5 and CMIP6 model simulations in comparison with the CORE-II simulations. First, the skill of the models' response, when forced by observed time series of the chlorofluorocarbon (CFC) distributions in the atmosphere, with regards to both surface distributions as well as vertical sections and global inventories will be assessed. Then, what controls different uptakes in the models and connections with overturning patterns will be investigated. OMIP re-enforces the recommendation that groups participating in CORE and OMIP implement CFCs and ideal age, following the CORE-II forcing protocol.

A CORE-II data archive containing monthly-mean output files from many of the models participated in the CORE-II effort is provided by NCAR and can be contributed to and accessed using Globus. The archive stores model fields on the models' native grids, using their own variable names in NetCDF format.

The Ocean Model Intercomparison Project (OMIP)

The CORE-II framework has reached a relatively mature state. Specifically, it is widely recognized as the community standard for global ocean – sea-ice simulations, and it is being adopted

by many groups worldwide for the evaluation of ocean and sea-ice components of their coupled models. The CORE-II framework and experiments are now included in the CMIP6 as an endorsed project, i.e., OMIP. OMIP aims to provide a framework for evaluating, understanding, and improving the ocean and sea-ice components of global climate and earth system models contributing to the CMIP6. OMIP addresses these aims in two complementary ways: by providing an experimental protocol for global ocean – sea-ice models run with a prescribed atmospheric forcing; and by providing a protocol for ocean diagnostics to be saved as part of CMIP6.

The Panel reviewed and discussed the physical component of the OMIP protocol design and ocean diagnostic archival plans, to support the finalization of the Griffies et al. (2016) OMIP overview article that provides full details on both. The physical portion of the OMIP experimental protocol follows that of the CORE-II experiments. We note that OMIP includes the previously separate Ocean Carbon Model Intercomparison Project (OCMIP). The related protocol, requested data sets, and relevant forcing information will be detailed in a separate publication led by James Orr of IPSL. This merging of ocean physical, chemical, and biogeochemical efforts into a single project allows for efficient communications across these communities participating in CMIP6.

The OMIP diagnostic protocol is relevant for any ocean model component of CMIP6, including the DECK (Diagnostic, Evaluation and Characterization of Klima experiments), historical simulations, FAFMIP (Flux Anomaly Forced MIP), C4MIP (Coupled Carbon Cycle Climate MIP), DAMIP (Detection and Attribution MIP), DCP (Decadal Climate Prediction Project), ScenarioMIP (Scenario MIP), as well as the ocean – sea-ice OMIP simulations. The bulk of the Griffies et al. (2016) paper offers scientific rationale for saving these diagnostics.

OMDP at the CLIVAR Open Science Conference (OSC)

All lead authors of the CORE-II papers were solicited – and they subsequently agreed – each prepare a poster for a CORE-II poster cluster at the CLIVAR OSC. OMDP will hold an open panel meeting on Saturday (17 September 2016) in Qingdao ahead of the OSC, focusing on the “finalization” of the JRA-55 data sets. OMDP members will also attend sessions held by the CLIVAR GSOP, CDP, ARP, PRP, and SORP, and the DCVP and EBUS Research Foci.

Acknowledgment

The OMDP would like to express its gratitude to Anna Pirani for her dedication and tireless efforts as the CLIVAR Project Office science liaison to OMDP. Anna has taken on a new position as the head of the IPCC WG1 Technical Support Unit. She played a critical role in the success of the OMDP (formerly Working Group on Ocean Model Development, WGOMD) and will be greatly missed!

References

- Compo, G. P., and Co-authors, 2011: The twentieth century reanalysis project. *Q.J.R. Meteorol. Soc.*, 137, 1–28.
- Griffies, S. M., and Co-authors, 2009: Coordinated Ocean-ice Reference Experiments (COREs). *Ocean Modell.*, 26, 1–46.
- Griffies, S. M., and Co-authors, 2016: Experimental and diagnostic protocol for the physical component of the CMIP6 Ocean Model Intercomparison Project (OMIP). *Geosci. Model Dev. Discuss.*, doi:10.5194/gmd-2016-77 (submitted).

ICPO, 2015: CLIVAR Ocean Model Development Panel (OMDP) mini workshop on forcing ocean and sea-ice models. CLIVAR Publication Series No. 202, 21 pp (Available from <http://www.clivar.org/documents/report-clivar-ocean-model-development-panel-omdp-mini-workshop-forcing-ocean-and-sea-ice>)

ICPO, 2016: Report of the 2nd Session of the CLIVAR Ocean Model Development Panel. CLIVAR Publication Series No. 210, 15 pp (Available from <http://www.clivar.org/documents/report-2nd-session-clivar-ocean-model-development-panel>)

Kobayashi, S. and Co-authors, 2015: The JRA-55 Reanalysis: General specifications and basic characteristics. *J. Meteorol. Soc. Japan*, 93, 5-48, doi: 10.2151/jmsj.2015-001.

Large, W. G., and S. G. Yeager, 2004: Diurnal to decadal global forcing for ocean and sea-ice models: The data sets and flux climatologies. NCAR Technical Note TN-460+STR, 105 pp.

Large, W. G., and S. G. Yeager, 2009: The global climatology of an interannually varying air-sea flux data set. *Clim. Dyn.*, 33, 341-364, doi:10.1007/s00382-008-0441-3.

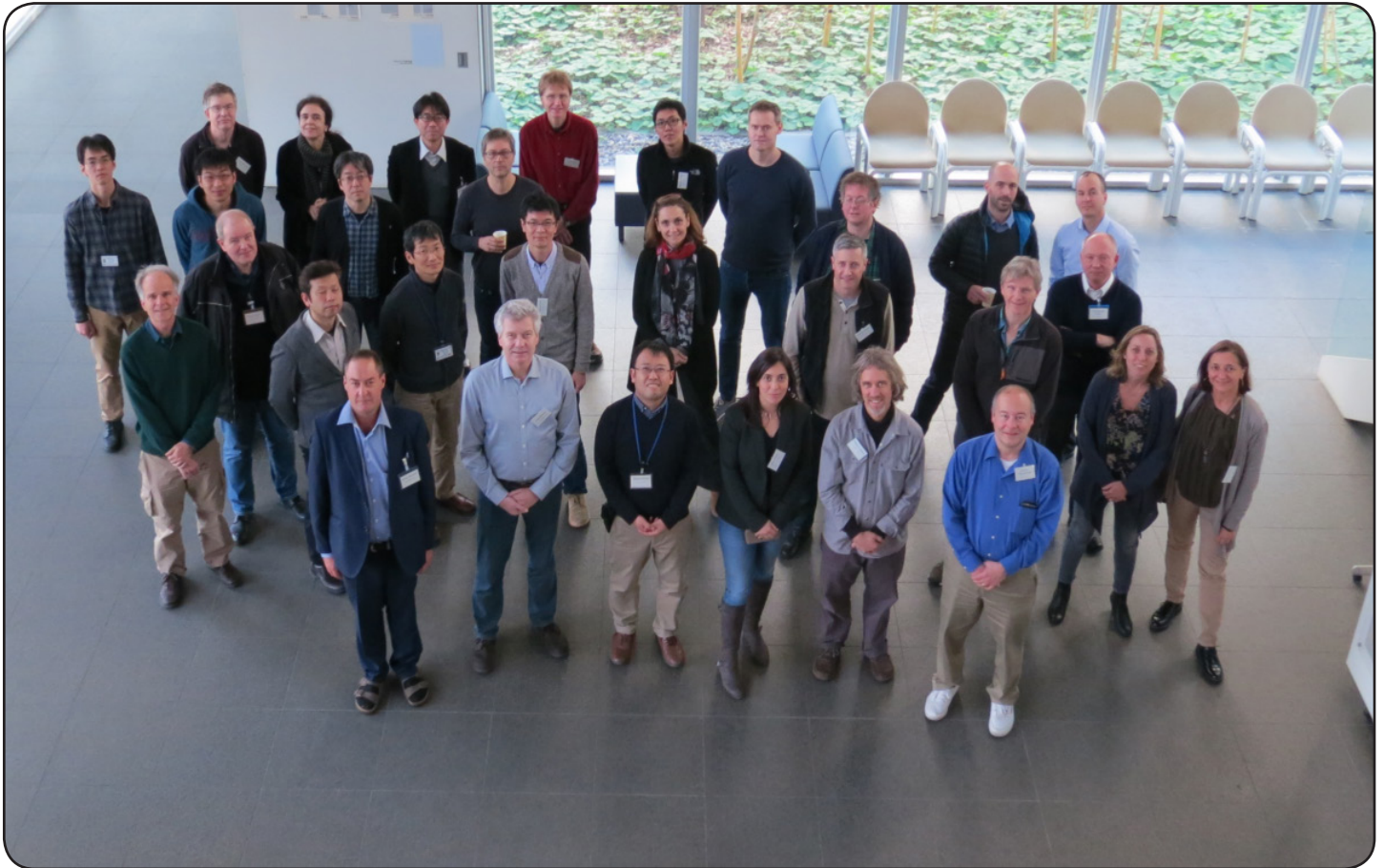


Figure: Participants of the 2nd Session of the CLIVAR Ocean Model Development Panel (OMDP), Yokohama, Japan

CONTENTS

Editorial	01
CLIVAR/JAMSTEC Workshop on the Kuroshio Current and Extension System: Theory, Observations, and Ocean Climate Modelling-The Workshop Overview and Outcomes Yoshiki Komuro, Gokhan Danabasoglu, Simon Marsland, Xiaopei Lin, Shoshiro Minobe, Anna Pirani, Tatsuo Suzuki, Ichiro Yasuda.....	01
Inter-Decadal Modulations in the Dynamical State of the Kuroshio Extension System: 1905-2015 Bo Qiu, Shuiming Chen, and Niklas Schneider.....	06
Variability and Mixing in the Kuroshio and Impact on Ecosystem and Climate Ichiro Yasuda.....	09
Observations of the Kuroshio Extension by an Autonomous Microstructure Float Takeyoshi Nagai, Ryuichiro Inoue, Amit Tandon, Hidekatsu Yamazaki.....	13
Observational and Numerical Study of the Frontal- and Mesoscale Air-Sea Interaction in the Kuroshio Extension Region in the North Pacific Xiaopei Lin, Xiaohui Ma, Zhaohui Chen, Lixiao Xu, Xue Liu, Zhao Jing, Lixin Wu, Dexing Wu, Ping Chang....	16
Effects of Deep Bottom Topography on the Kuroshio Extension Studied by a Nested-grid OGCM Masao Kurogi, Yukio Tanaka, and Hiroyasu Hasumi	19
An Extra Product of the JRA-55 Atmospheric Reanalysis and In Situ Observations in the Kuroshio-Oyashio Extension Under the Japanese “Hotspot Project” Hisashi Nakamura, Yoshimi Kawai, Ryusuke Masunaga, Hirotaka Kamahori, Chiaki Kobayashi and Makoto Koike.....	22
Mesoscale Imprints of the Kuroshio Extension and Oyashio Fronts on the Wintertime Atmospheric Boundary Layer Ryusuke Masunaga, Hisashi Nakamura, Takafumi Miyasaka, Kazuaki Nishii, Youichi Tanimoto, Bo Qiu.....	27
Where’s the Data? Meghan F. Cronin.....	31
Summary of the 2nd Session of the CLIVAR Ocean Model Development Panel (OMDP) - Extended Meeting on Forcing Ocean-Ice Climate Models Anna Pirani, Gokhan Danabasoglu, Simon Marsland.....	32



The CLIVAR Exchanges is published by the International CLIVAR Project Office
ISSN No: 1026-0471

Editor: Nico Caltabiano (CLIVAR)
Guest editors: Yoshiki Komuro (JAMSTEC)

Layout: Harish J. Borse, ICMPO at IITM, Pune, India
Production, Printing and Mailing by the ICMPO with support of IITM and the Indian Ministry of Earth Sciences.



सत्यमेव जयते
Ministry of Earth Sciences

Note on Copyright:

Permission to use any scientific material (text as well as figures) published in CLIVAR Exchanges should be obtained from the authors. The reference should appear as follows: Authors, Year, Title. CLIVAR Exchanges, No.pp. (Unpublished manuscript).

The ICPO is supported by

China State Oceanographic Administration /First Institute of Oceanography (FIO), Indian Ministry of Earth Sciences/ Indian Institute of Tropical Meteorology (IITM) and NASA, NOAA, NSF and DoE through US CLIVAR.

WCRP is sponsored by the World Meteorological Organization, the International Council for Science and the Intergovernmental Oceanographic Commission of UNESCO.

Contact:

Executive Director, ICPO
First Institute of Oceanography, SOA, 6 Xianxialing Road, Laoshan District, Qingdao 266061, China
icpo@clivar.org
http://www.clivar.org



Please recycle this newsletter by passing on to a colleague or library or disposing in a recognised recycle point